Selective Oxidation of H_2S in Biogas to Sulfur on V_2O_5 Catalyst Dispersed on CeO_2-MO_2 (M = Ti, Si, Zr) Mixed Oxides

Miss Benjamaporn Tudkesorn

จุฬาลงกรณ์มหาวิทยาลัย
CHULALONGKORN UNIVERSITY

A Thesis Submitted in Partial Fulfillment of the Requirements

for the Degree of Master of Engineering in Chemical Engineering

Department of Chemical Engineering

FACULTY OF ENGINEERING

Chulalongkorn University

Academic Year 2019

Copyright of Chulalongkorn University

ปฏิกิริยาออกซิเดชันแบบเลือกเกิดของไฮโดรเจนซัลไฟด์ในไบโอแก๊สเป็นซัลเฟอร์
บนตัวเร่งปฏิกิริยา V_2O_5 ที่กระจายตัวบนออกไซด์ผสม CeO_2-MO_2 (M = Ti, Si, Zr)

น.ส.เบญจมาภรณ์ ทัศเกษร

Thesis Title   Selective Oxidation of H_2S in Biogas to Sulfur on V_2O_5 Catalyst Dispersedon CeO_2-MO_2 (M = Ti, Si, Zr) Mixed Oxides

By   Miss Benjamaporn Tudkesorn

Field of Study   Chemical Engineering

Thesis Advisor   Professor JOONGJAI PANPRANOT, Ph.D.

Accepted by the FACULTY OF ENGINEERING, Chulalongkorn University in Partial Fulfillment of the Requirement for the Master of Engineering

-- Dean of the FACULTY OF ENGINEERING

(Associate Professor SUPOT TEACHAVORASINSKUN, Ph.D.)

THESIS COMMITTEE

-- Chairman

(AKAWAT SRIRISUK, Ph.D.)

-- Thesis Advisor

(Professor JOONGJAI PANPRANOT, Ph.D.)

-- Examiner

(Assistant Professor PALANG BUMROONGSAKULSAWAT, Ph.D.)

-- External Examiner

(Assistant Professor Soipatta Soisuwan, Ph.D.)

เบญจมาภรณ์ ทัศเกษร : ปฏิกิริยาออกซิเดชันแบบเลือกเกิดของไฮโดรเจนซัลไฟด์ในไบโอแก๊สเป็นซัลเฟอร์บนตัวเร่งปฏิกิริยา V_2O_5 ที่กระจายตัวบนออกไซด์ผสม CeO_2-MO_2 (M = Ti, Si, Zr). (Selective Oxidation of H_2S in Biogas to Sulfur on V_2O_5 Catalyst Dispersedon CeO_2-MO_2 (M = Ti, Si, Zr) Mixed Oxides) อ.ที่ปรึกษาหลัก : ศ.จูงใจ ปั้นประณต

งานวิจัยนี้ศึกษาคุณลักษณะและประสิทธิภาพของตัวเร่งปฏิกิริยาวาเนเดียมบนตัวรองรับแบบออกไซด์ผสมระหว่างซีเรีย-ออกไซด์ของโลหะ (ไททาเนียม ซิลิคอน และเซอร์โคเนียม) เปรียบเทียบกับตัวรองรับซีเรียเกรดการค้าในปฏิกิริยาออกซิเดชันแบบเลือกเกิดของไฮโดรเจนซัลไฟด์ในไบโอแก๊สเป็นซัลเฟอร์ที่อุณหภูมิ 130 องศาเซลเซียส เตรียมตัวรองรับออกไซด์ผสมซีเรียต่างๆด้วยวิธีตกตะกอนร่วม โดยมีปริมาณวาเนเดียม ๓ เปอร์เซ็นโดยน้ำหนักบนตัวรองรับ เตรียมด้วยวิธีเคลือบฝังแบบเปียก จากการวิเคราะห์ด้วยเทคนิคการกระเจิงรังสีเอ็กซ์และรามานสเปกโตรสโกปีพบว่าตัวเร่งปฏิกิริยาทุกตัวมีการกระจายตัวของวาเนเดียมบนตัวรองรับสูง โดยตัวเร่งปฏิกิริยาวาเนเดียมบนตัวรองรับแบบออกไซด์ผสมด้วยซิลิกาในอัตราส่วน 1 ต่อ 1 โมลาร์ของออกไซด์โลหะมีประสิทธิภาพดีที่สุด แสดงค่าการเปลี่ยนแปลงร้อยละของแก๊สไฮโดรเจนซัลไฟด์สูง (73%) และการเลือกเกิดของแก๊สซัลเฟอร์ไดออกไซด์ต่ำ (19 ppm) จากการวิเคราะห์ด้วยเทคนิคการคายซับของออกซิเจน พบว่าอันตรกิริยาที่แข็งแรงระหว่างวาเนเดียมเพนตะออกไซด์และตัวรองรับทำให้เกิดช่องว่างระหว่างออกซิเจนมากขึ้น ทั้งนี้ ตัวเร่งปฏิกิริยา V_2O_5/CeO_2-SiO_2 สามารถคายซับแก๊สออกซิเจนได้ที่อุณหภูมิต่ำสนับสนุนให้ตัวเร่งปฏิกิริยาคืนสภาพจาก V^{4+} เป็น V^{5+} ได้เร็ว ซึ่งมีผลโดยตรงต่อขั้นตอนกำหนดอัตราเร็วของปฏิกิริยาออกซิเดชันแบบเลือกเกิดของไฮโดรเจนซัลไฟด์ทำให้อัตราการเกิดปฏิกิริยาสูงขึ้น

สาขาวิชา	วิศวกรรมเคมี	ลายมือชื่อนิสิต
		....
ปี	2562	ลายมือชื่อ อ.ที่ปรึกษาหลัก
การศึกษา		....

6170203321 : MAJOR CHEMICAL ENGINEERING

KEYWORD:

Benjamaporn Tudkesorn : Selective Oxidation of H_2S in Biogas to Sulfur on V_2O_5 Catalyst Dispersedon CeO_2-MO_2 (M = Ti, Si, Zr) Mixed Oxides. Advisor: Prof. JOONGJAI PANPRANOT, Ph.D.

In this research, the characteristics and catalytic performances of V_2O_5 catalysts supported on mixed oxides CeO_2-MO_2 (M = Ti, Si, Zr) as compared to the commercial CeO_2 supported ones were studied in the selective catalytic oxidation of H_2S in biogas to sulfur at $130^{\circ}C$. The mixed-oxide supports were prepared by co-precipitation method with 3 wt.% vanadium loading by wet impregnation method. From the XRD and Raman spectroscopy results, all the catalysts exhibited high dispersion of V_2O_5 on the supports with the 1:1 molar ratio CeO_2-SiO_2 mixed oxide showed the highest conversion of H_2S at 73% and low selectivity of SO_2 at 19 ppm. From the O_2-TPD results, the strong interaction between V_2O_5 and support produced more oxygen vacancies and as a consequence, the V_2O_5/CeO_2-SiO_2 exhibited low temperature desorption peak of chemically adsorbed oxygen suggesting a rapid restoration of catalyst from V^{4+} to V^{5+} state, which was directly related to the limiting step of the selective oxidation of H_2S. As a consequence, the catalyst activity could be enhanced.

Field of Study:	Chemical Engineering	Student's Signature
		....
Academic Year:	2019	Advisor's Signature
		....

ACKNOWLEDGEMENTS

จุฬาลงกรณ์มหาวิทยาลัย

CHULALONGKORN UNIVERSITY

TABLE OF CONTENTS

LIST OF TABLES

LIST OF FIGURES

CHAPTER I

INTRODUCTION

1.1 Introduction

Biofuel or biogas is an eco-friendly for energy production. It is naturally the decompose of organic, food and animal waste, in an anaerobic environment and is now becoming an important source of green and clean energy [1]. Biogas contains mainly two compounds are methane (CH_4) and carbon dioxide (CO_2) in different percentages depending on the source of decompose. There are 0-1% composition of other components such as hydrogen sulfide (H_2S), hydrogen (H_2), nitrogen (N_2), oxygen (O_2), carbon monoxide (CO) and ammonia (NH_3) [2, 3].

The presence of H_2S strongly affects the use of biogas in equipment directly and indirectly by the means of contraction between H_2S and moisture which results in sulfuric acid. For the carbon steel and alloyed steel, the corrosion rate by H_2S is around 0.1-1 mm/year to the wall. In case of combination of H_2S and moisture, the corrosion rate by sulfuric acid was 1-3 mm/year to the wall of carbon steels. The corrosive tendency effect increases when temperature increases, at temperature of 100 $^\circ$C it exceeds 10 mm/year. Therefore, In order to protect the equipment, H_2S must be removed from biogas before entering to the process [4].

The most popular conversion method used for removal of H_2S is the Claus process which involves burning of the H_2S in air at high temperature of 980-1540 $^\circ$C and high pressure of 70 kPa. The selective H_2S catalytic oxidation is an interesting alternative method for H_2S removal because it operates at low temperature and low pressure [5-7].

Total oxidation of H_2S is following reaction (1) : [8]

$$2H_2S + 3O_2 \quad \longrightarrow \quad 2H_2O + 2SO_2 \quad \text{-------------------- (1)}$$
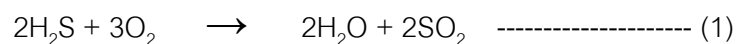
Selective oxidation of H_2S to sulfur element is following reaction (2)-(5): [9]

Main reaction $\quad H_2S + \frac{1}{2}O_2 \quad \longrightarrow \quad 1/nS_n + H_2O \quad$ -------------------- (2)

Side reaction $\quad H_2S + 3/2O_2 \quad \longrightarrow \quad SO_2 + H_2O \quad$ -------------------- (3)

$\quad\quad\quad\quad\quad\quad 1/nS_n + O_2 \quad \longrightarrow \quad SO_2 \quad\quad\quad\quad$ -------------------- (4)

$\quad\quad\quad\quad\quad\quad 3/nS_n + 2H_2O \quad \longleftrightarrow \quad H_2S + SO_2 \quad$ -------------------- (5)
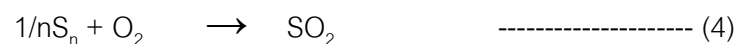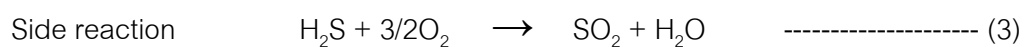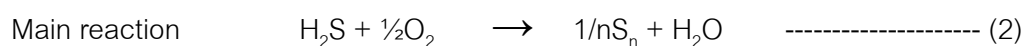
Vanadium-based catalysts have been reported to be active for selective catalytic oxidation of hydrogen sulfide (H_2S) to sulfur [10-13]. A series of CeO_2-MO_2 (M = Ti^{4+}, Si^{4+} and Zr^{4+}) supported vanadium catalyst were investigated and V_2O_5/CeO_2 showed better performance compared with TiO_2 and $CuFeO_4$ [8]. In this experiment, CeO_2-based mixed metal oxide were prepared and employed as the supports for preparation of supported V_2O_5 catalysts in the selective oxidation of H_2S to sulfur compound.

In this research, we aim to study the characteristics and catalytic activity of V_2O_5 dispersed on pure CeO_2 and CeO_2-MO_2 mixed oxide supports prepared with different molar ratios between CeO_2 and MO_2 in the selective oxidation of H_2S to sulfur element. This research contains three parts of studies: first, preparation the mixed-metal oxide supports, CeO_2-TiO_2, CeO_2-SiO_2 and CeO_2-ZrO_2 using co-precipitation method and preparation of 3 wt.% of V_2O_5 supported on CeO_2-MO_2 using impregnation method: second, the properties and characteristics of catalysts analyzed by X-ray diffraction (XRD), Raman spectroscopy, N_2-physisorption, Inductively coupled plasma-optical emission spectrometry (ICP-OES), Scanning electron microscopy with energy dispersive X-ray spectroscopy (SEM-EDX), Fourier transforms infrared spectroscopy (FT-IR), X-ray photoelectron spectroscopy (XPS) and Oxygen-Temperature programmed desorption (O_2-TPD). And the last part is the catalytic activity test were carried out in H_2S oxidation at 130°C and atmospheric pressure.

1.2 Objectives of the Research

To study the characteristics and catalytic performances of CeO_2 and CeO_2-MO_2 (M = Ti, Si, Zr) supported V_2O_5 in the selective catalytic oxidation of H_2S.

1.3 Scope of the Research

1.3.1 To study the characteristics and catalytic performances of CeO_2 and CeO_2-MO_2 (M = Ti, Si, Zr) supported V_2O_5 in the selective catalytic oxidation of H_2S

1) Preparation of CeO_2-MO_2 with 1:1 molar ratio (M = Ti, Si, Zr) support by co-precipitation method and calcined at 500°C for 5 h in air with 10°C/min of ramp rate on temperature.

2) Preparation of 3 wt.% V_2O_5 over CeO_2 and CeO_2-MO_2 (M = Ti, Si, Zr) catalyst by wet impregnation method and calcined at 500°C for 5 h in air with 10°C/min of ramp rate on temperature.

3) The catalysts were pretreated with helium at 200°C for 1 h before reaction tests.

4) The catalytic activity tests were carried out in selective oxidation of H_2S at 130°C and atmospheric pressure with 0.5 of O_2/H_2S ratio.

5) Characterization of the prepared catalysts by various method following

5.1) X-ray diffraction (XRD)

5.2) Raman spectroscopy

5.3) N_2-physisorption

5.4) Inductively coupled plasma-optical emission spectrometry (ICP-OES)

5.5) Scanning electron microscopy with energy dispersive X-ray spectroscopy (SEM-EDX)

5.6) Fourier transforms infrared spectroscopy (FT-IR)

5.7) Oxygen-Temperature programmed desorption (O_2-TPD)

5.8) X-ray photoelectron spectroscopy (XPS)

1.3.2 The best catalyst from above study was selected to study the effect of mixing molar ratio between CeO_2 and MO_2 support on catalytic performance for selective catalytic oxidation of H_2S.

1) Preparation of CeO_2-MO_2 with desired molar ratio support by co-precipitation method and calcined at 500°C for 5 h in air with 10°C/min of ramp rate on temperature.

2) Preparation of 3 wt.% V_2O_5 over mixed oxide support catalyst by wet impregnation method and calcined at 500°C for 5 h in air with 10°C/min of ramp rate on temperature.

3) The catalysts were pretreated with helium at 200°C for 1 h before reaction tests.

4) The catalytic activity tests are carried out in selective oxidation of H_2S at 130°C and atmospheric pressure with 0.5 of O_2/H_2S ratio.

5) Characterization of the prepared catalysts by various method following

    5.1) X-ray diffraction (XRD)

    5.2) Raman spectroscopy

    5.3) N_2-physisorption

    5.4) Inductively coupled plasma-optical emission spectrometry (ICP-OES)

    5.5) Scanning electron microscopy with energy dispersive X-ray spectroscopy (SEM-EDX)

    5.6) Fourier transforms infrared spectroscopy (FT-IR)

    5.7) Oxygen-Temperature programmed desorption (O_2-TPD)

    5.8) X-ray photoelectron spectroscopy (XPS)

1.4 Research Methodology

1.4.1 To study the characteristic and catalytic performance of CeO_2 and CeO_2-MO_2 (M = Ti, Si, Zr) supported V_2O_5 in the selective catalytic oxidation of H_2S

```
┌─────────────────────────┐          ┌──────────────────────────────────┐
│   Support preparation   │──────────│ Preparation of CeO₂- MO₂ with 1:1 │
└─────────────────────────┘          │ molar ratio base on oxides support │
              │                      │ by co-precipitation method         │
              ▼                      │                                    │
┌─────────────────────────┐          │      ● CeO₂                        │
│   Catalyst preparation  │          │      ● CeO₂-TiO₂                    │
└─────────────────────────┘          │      ● CeO₂-SiO₂                    │
              │                      │      ● CeO₂-ZrO₂                     │
              ▼                      └──────────────────────────────────┘
```

Support preparation

Catalyst preparation

Preparation of CeO_2- MO_2 with 1:1 molar ratio base on oxides support by co-precipitation method

- CeO_2
- CeO_2-TiO_2
- CeO_2-SiO_2
- CeO_2-ZrO_2

Preparation of 3 wt.% V_2O_5 over CeO_2 and CeO_2-MO_2 catalyst by wet impregnation method

- 3%V_2O_5/CeO_2 (VC)
- 3%V_2O_5/CeO_2-TiO_2 (VCT)
- 3%V_2O_5/CeO_2-SiO_2 (VCS)
- 3%V_2O_5/CeO_2-ZrO_2 (VCZ)

The catalyst was pretreated with helium at 200°C for 1 h before reaction tests.

The catalytic activity tests are carried out in selective oxidation of H_2S at 130°C and atmospheric pressure with 0.5 of O_2/H_2S ratio.

Discussions and conclusions

Catalyst characterizations by

- XRD
- Raman
- N_2-physisorption
- ICP-OES
- SEM-EDX
- FT-IR
- O_2-TPD
- XPS

1.4.2 The best catalyst from above study was selected to study the effect of mixing molar ratio between CeO_2 and MO_2 (SiO_2 and TiO_2) support on catalytic performance for selective catalytic oxidation of H_2S.

```
┌─────────────────────┐        ┌──────────────────────────────┐
│ Support preparation │────────│ Preparation of CeO₂-SiO₂ with│
└─────────────────────┘        │ CeO₂/SiO₂ = 1/2, 1/3, 2/1 and│
           │                   │ 3/1 and CeO₂-TiO₂ with CeO₂/ │
           ▼                   │ TiO₂ = 1/2 and 2/1 molar     │
┌─────────────────────┐        │ ratio by co-precipitation    │
│ Catalyst preparation│        │ method.                      │
└─────────────────────┘        └──────────────────────────────┘
```

Support preparation → Catalyst preparation

Preparation of CeO₂-SiO₂ with CeO₂/SiO₂ = 1/2, 1/3, 2/1 and 3/1 and CeO₂-TiO₂ with CeO₂/TiO₂ = 1/2 and 2/1 molar ratio by co-precipitation method.

Preparation of 3 wt.% V_2O_5 over CeO_2-SiO_2 catalyst by wet impregnation method

- $3\%V_2O_5/CeO_2$-SiO_2 (VCS12, VCS13, VCS21 and VCS31)
- $3\%V_2O_5/CeO_2$-TiO_2 (VCT12 and VCT21)

The catalyst was pretreated with helium at 200°C for 1 h before reaction tests.

The catalytic activity tests are carried out in selective oxidation of H_2S at 130°C and atmospheric pressure with 0.5 of O_2/H_2S ratio.

Discussions and conclusions

Catalyst characterizations by

- XRD
- Raman
- N_2-physisorption
- ICP-OES
- SEM-EDX
- FT-IR
- O_2-TPD
- XPS

CHAPTER II

BACKGROUND AND LITERATURE REVIEW

2.1 Biogas

Biofuel or biogas is an eco-friendly for energy production. It is naturally decomposition in decompose of organic, food and animal waste, in an anaerobic environment become too important source of green and clean energy, yielding 5.5-7 kWh.m^{-3}. The energy directly depends on methane content [1, 14]. Biogas contains mainly two compounds are methane (CH_4) and carbon dioxide (CO_2) in difference percentage depend on source of decompose. There are 0-1% composition of each other components such as hydrogen sulfide (H_2S), hydrogen (H_2), Nitrogen (N_2), Oxygen (O_2), carbon monoxide (CO) and ammonia (NH_3) [2].

Table 1 Typical composition (%) of biogas [2].

Component	Agricultural waste	Landfills	Industrial waste
Methane (CH_4)	50-80	50-80	50-70
Carbon dioxide (CO_2)	30-50	20-50	30-50
Hydrogen sulfide (H_2S)	0.70	0.10	0.80
Hydrogen (H_2)	0-2	0-5	0-2
Nitrogen (N_2)	0-1	0-3	0-1
Oxygen (O_2)	0-1	0-1	0-1
Carbon monoxide (CO)	0-1	0-1	0-1
Ammonia (NH_3)	Trace	Trace	Trace

2.2 Hydrogen sulfide (H_2S)

The extremely hazardous hydrogen sulfide (H_2S) gas is colorless and flammable with a strongly rotten egg smell although the concentration of H_2S is very low in air. H_2S occurs naturally in petroleum crude oil, natural gas, biomass decomposition and hot spring [15]. However, is available in the processing industry such as refinery industry, heavy and metal industry, pulp and paper industry, chemical industry and public utilities i.e. bacteriological composing of west and dewatering of sewage sludge [16].

Health effects of H_2S are both irritation, block sense of smell and interrupt cells from receiving oxygen. The toxic limitation value that immediately dangerous to life and health is 100 ppm of H_2S concentration [16].

Table 2 Specifications of H_2S [16].

Synonyms	Hydrogen sulfide
	Hydrosulfuric acid
	Sulfane
	Dihydrogen monosulfide
Molecular Formula	H_2S
Molecular weight	34.08 g/mol
Density	0.002 g/mL (at 68 $^\circ$F / 20 $^\circ$C)
Ignition temperature	518 $^\circ$F / 270 $^\circ$C
Melting point	-122.08 $^\circ$F / -85.6 $^\circ$C
Boiling point	-76.36 $^\circ$F / -60.2 $^\circ$C
UEL	45.5 Vol.%
LEL	4.3 Vol.%
Hazard symbols	

The effect of H_2S on the equipment directly and indirectly by the means of contraction between H_2S and moisture result to sulfuric acid. For the carbon steel and alloyed steel, the corrosion rate by H_2S affect 0.1-1 mm/year to the wall. In the case of combination of H_2S and moisture, the corrosion rate by sulfuric acid affect 1-3 mm/year to the wall of carbon steels. The corrosive tendency effect increases when temperature increases, at temperature of 100 $^\circ$C it exceeds 10 mm/year. Therefore, In order to protect the equipment, H_2S must be removed from biogas before entering to the process [4].

The most popular conversion method used to remove H_2S is the Claus process which involves hydrogen sulfide burning in air at high temperature of 980-1540 $^\circ$C and high pressure of 70 kPa. The other alternative is selective H_2S catalytic oxidation, was operated at low temperature and low pressure [7].

2.3 Elimination of hydrogen sulfide [7, 17]

Claus process is the most common used to recover the hydrogen sulfide and converted to sulfur element. Claus process also consist of multistage following:

1) Thermal oxidation

$$2H_2S + 3O_2 \longrightarrow 2SO_2 + 2H_2O + heat \qquad \text{-------------------- (6)}$$
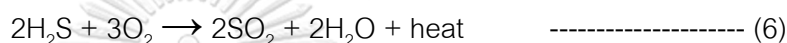
One-third of hydrogen sulfide (H_2S) is burning with air to generate sulfur dioxide (SO_2) at temperature of 980-1540 $^\circ$C and higher pressure of 70 kPa.

2) Catalytic reaction

$$2H_2S + 3SO_2 \longrightarrow 3S + 2H_2O + heat \qquad \text{-------------------- (7)}$$
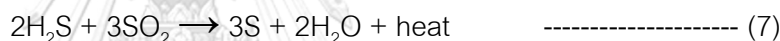
Two-third remaining unconverted of hydrogen sulfide (H_2S) reacts with sulfur dioxide to produce sulfur element through the subsequent catalytic reaction at temperature of 200-315 $^\circ$C. From the limitation in chemical equilibrium reaction, 3-5% of H_2S cannot converted to sulfur element. So, it is necessary to treat the residual gas of the Claus process by another techniques such as adsorption wet catalytic reaction and catalytic reaction.
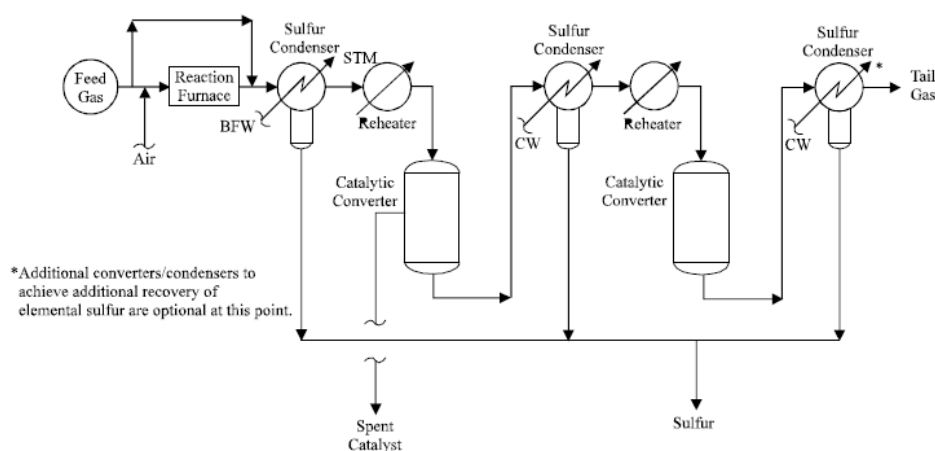
Figure 1 Claus sulfur recovery unit diagram [18].

The importance developed processes to treat the residual gas from Claus process are Mobil direct oxidation process (MODOP) and Super Claus process. The principles of two processes are based on the irreversible selective oxidation of H_2S [19].

Total oxidation of hydrogen sulfide is following reaction (8): [8]

$$2H_2S + 3O_2 \longrightarrow 2H_2O + 2SO_2 \qquad \text{--------------------- (8)}$$

Selective oxidation of hydrogen sulfide to sulfur element is responded following reaction (9)-(12): [9]

Main reaction	$H_2S + \frac{1}{2}O_2$	$\longrightarrow$	$1/nS_n + H_2O$	-------------------- (9)
Side reaction	$H_2S + 3/2O_2$	$\longrightarrow$	$SO_2 + H_2O$	------------------ (10)
	$1/nS_n + O_2$	$\longrightarrow$	SO_2	------------------ (11)
	$3/nS_n + 2H_2O$	$\longleftrightarrow$	$H_2S + SO_2$	------------------ (12)
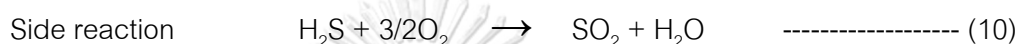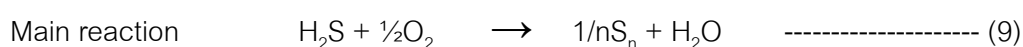
2.4 Vanadium pentoxide

Vanadium pentoxide (V_2O_5) appears as a yellow to rust-brown crystalline powder and slightly soluble in water. Vanadium pentoxide is popularly used in oxidation catalyst both homogeneous and heterogeneous processes for many industries such as the sulfuric acid production from sulfur dioxide, adipic from cyclohexanol and acetaldehyde from alcohol. The preparation of vanadium pentoxide also involves the ammonium metavanadate decomposition at temperature of 500-550°C [20, 21].
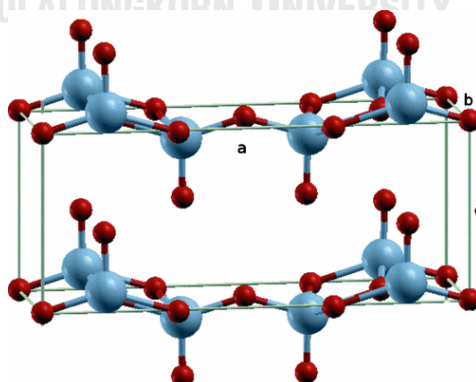
Figure 2 Vanadium pentoxide [22]

Table 3 Physical/chemical properties of vanadium pentoxide [23]

Synonyms	Vanadium (V) oxide
	Divanadium pentoxide
Molecular Formula	V_2O_5
Molecular weight	181.88 g/mol
Density	3.357 g/cm^3
Flash point	Non-flamable
Melting point	690°C
Boiling point	1,750°C (decompose)
Solubility in water	0.8 g/L at 20°C
Hazard symbols	

Davydov et al. (2003) [10] Study the catalytic activity of 12 metal oxides (MgO, TiO_2 ZrO_2, V_2O_5, Mn_2O_3, Cr_2O_3, Fe_2O_3, CuO, CoO, Al_2O_3, Sb_6O_{13} and Bi_2O_3) in selective oxidation of H_2S by molecular of oxygen to propose for sulfur selective production. V_2O_5 is the most active catalyst for the selective catalytic oxidation of H_2S to give high conversion of H_2S while BiO_3, Fe_2O_3 and CuO mainly carried out the SO_2 formation in complete oxidation of H_2S reaction.

Li et al (1996) [9] Study the catalytic activity of hydrogen sulfide selective oxidation over single oxide, the result shows that vanadium oxide had to be the best performance in H_2S conversion and sulfur selectivity. The catalytic activity decreased in the following iron oxide, bismusth oxide, molybdenum oxide and magnesium oxide respectively. In case of vanadium-based mixed oxide catalyst studied, consist of vanadium-molydenum (V/Mo = 1/0, 5/1, 2/1, 1/1, 2/7 and 0/1), vanadium-bismust (V/Bi = 1/0, 2/1, 1/1, 1/2 and 0/1) and vanadium-magnesium (V/Mg = 1/0, 3/1, 1/1, 1/3 and 0/1). the addition of Mo, Bi and Mg significantly improve the catalytic performance due to exhibits strong synergistic behavior.

Kim et al (2006) [24] The selective oxidation of hydrogen sulfide containing excess water and ammonia were studied over the V_2O_5/TiO_2 aerogel catalyst. The aerogel catalyst with 2 wt.% of vanadium oxide showed the highest surface area compared with higher content of vanadium (5 wt.% and 10 wt.%). The comparison between V_2O_5/TiO_2 aerogel and xerogel catalyst, aerogel catalyst exhibited on higher conversion of H_2S without SO_2 formation.

Soriano et al (2015) [5] V_2O_5 supported on porous clay heterostructure (PCH) catalysts were studied for the partial oxidation of H_2S. The catalyst with higher V_2O_5 content are more active, a higher of H_2S conversion and SO_2 selectivity, and resistance to the deactivation.

Soriano et al (2009) [25] V_2O_5 supported on mesoporous zircronium phosphate (MZP) catalyst were studied for the selective oxidation of H_2S. The catalytic activity and stability increasing with the V-loading and sulfur deposit on the catalyst is favored in catalyst with low V-loading.

Pongthawornsakun et al (2018) [12] TiO_2 supported vanadium oxide were investigated at 130 $^\circ$C for selective oxidation of H_2S. V_2O_5/TiO_2 (anatase) exhibited the best catalyst performance with 80% conversion of H_2S and low selectivity of SO_2 (<7 ppm). The highly dispersed vanadium oxide on the support result to partially reduced V-Ti species influenced the redox capability of V^{5+}/V^{4+}, directly affect to the limiting step of reaction.

2.5 Cerium (IV) oxide

Cerium (IV) oxide (CeO_2) appears as a yellow to white powder. CeO_2 is insoluble in water and moderately soluble in strong mineral acids. Ceria was used as a catalyst in automotive application and co-catalyst in many reaction such as Fischer-Tropsch reaction, selective oxidation and steam reforming of ethanol into carbondioxide and hydrogen. The structure of ceria is fluorite, oxygen atom are all in a plane which allows for rapid diffusion of the oxygen vacancies [26].
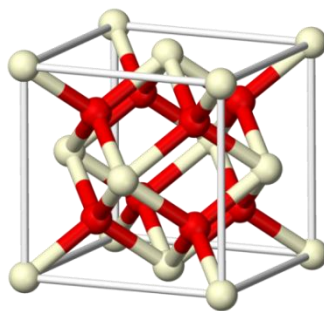
Figure 3 Cerium oxide [27]

Table 4 Physical/chemical properties of cerium oxide [26]

Synonyms	Cerium dioxide
	Ceria
Molecular Formula	CeO_2
Molecular weight	172.11 g/mol
Density	7.65 g/cm^3
Melting point	2,500 $^\circ$C
Boiling point	3,500 $^\circ$C
Solubility in water	Insoluble
Hazard symbols	

Barba et al (2013) [8] To compare the activity for selective catalytic H_2S oxidation, different vanadium (V_2O_5) based supported catalyst including TiO_2, CeO_2 and $CuFe_2O_4$ were studied. The surface area of the supported was decreased after V_2O_5 doped because V_2O_5 could be clogging in the pore of support but $V_2O_5/CuFe_2O_4$ wasn't observed the difference of surface area after V_2O_5 doped due to the initial specific surface area of $CuFe_2O_4$ is very low. At the reaction temperature of 250 $^\circ$C, the result has shown a higher conversion of H_2S and low selectivity of SO_2 at 3% on CeO_2 supported V_2O_5. From studied the effect of temperature on the reaction, it was found that the conversion of H_2S increase and selectivity of SO_2 decrease when reaction temperature increased.

Palma et al (2014) [11] To study the catalytic activity for selective catalytic H_2S oxidation of CeO_2 supported vanadium (V_2O_5) catalyst in different loading of V_2O_5. 2.55-20 wt.% loading of V_2O_5 on the support were characterized, the result showed increasing of vanadium content could lead to blocking and clogging in the pores of support result to decrease the surface area of catalyst. For 20 wt.% loading of V_2O_5, cerium vanadate ($CeVO_4$) can be observed at XRD peak of $2\Theta \sim 24°$, $32.4°$ and $33.1°$ due to the reaction between CeO_2 and V_2O_5 following:

$$CeO_2(s) + 0.5V_2O_5(s) \longrightarrow CeVO_4(s) + 0.5O_2(g) \qquad \text{------------------- (13)}$$
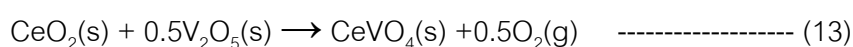
After catalytic activity test of 20 wt.% V_2O_5/CeO_2, the catalyst was a good activity with 99% of sulfur selectivity and 98.7% of H_2S conversion at 150 °C which very close to the calculation of thermodynamic equilibrium.

Zang et al (2013) [13] A series of vanadium supported on ceria doped with Lamponite clay catalyst was studied the structural and activity for selective oxidation of H_2S. V_2O_5/CeO_2-Lap is a mesoporous structure with high surface area. The emperature programed desorption technique was used to characterize the ability to adsorb and desorb O_2 of catalyst. The peak observed at 120 °C attributed to chemically adsorbed oxygen. The peak at 450 °C represented to desorption of oxygen molecule on the oxygen vacancies. For the 5% V_2O_5/CeO_2-Lap exhibits the largest peak, indicating that it is the largest of oxygen vacancies amount which agreeable with the result from the activity test. The maximum conversion of H_2S is 98% and yield of sulfur is 98% at 180 °C. In order to study the catalyst deactivated after reaction time for 7 h, catalyst as purge with the N_2 at 300 °C and then fed with 2% O_2. The experiments are shown the existence of Ce^{3+} could be resistant to the deactivation of catalyst.

Yasyerli et al (2006) [28] Ce-V mixed oxides have studied the activity for selective oxidation of H_2S to sulfur, Ce-V mixed oxide atomic ratio of one (Ce/V = 2/2) showed 100% H_2S conversion when O_2/H_2S feed ratios of 0.5 used at 250 °C. The selectivity of sulfur decreased with O_2/H_2S ratio increased to over the stoichiometric value.

2.6 Mixed metal oxide

Reddy et al (2004) [29] To investigate structural characteristics of a series of $V_2O_5/CeO_2\text{-}MO_2$ (M = Si^{4+}, Ti^{4+} and Zr^{4+}) with 1:1 molar ratio catalyst. The highest surface area found on $CeO_2\text{-}SiO_2$ support.

For the $CeO_2\text{-}SiO_2$, the result from XRD indicating that SiO_2 is an amorphous due to the peak of SiO_2 are absent. Calcination of catalyst at $500\,^{\circ}C$, $600\,^{\circ}C$ and $800\,^{\circ}C$ gave a good dispersion of V_2O_5, formation of $CeVO_4$ and formation of $Ce_{9.33}(SiO_4)_6O_2$ phase between CeO_2 and SiO_2 respectively. For the $CeO_2\text{-}TiO_2$, the result from XRD indicating that TiO_2 is an anatase phase with a few formation of $CeVO_4$ at calcination of $500\,^{\circ}C$. Calcination of catalyst at $800\,^{\circ}C$ and $1250\,^{\circ}C$, TiO_2 rutile phase and Ce-Ti oxides (Ce_2TiO_5, $Ce_2Ti_2O_7$ and $Ce_4Ti_9O_{24}$) could be found respectively. For the $CeO_2\text{-}ZrO_2$, the result from XRD showed $CeO_2\text{-}ZrO_2$ is a cubic fluorite-type with composition $Ce_{0.75}Zr_{0.25}O_2$ when calcined at $500\,^{\circ}C$. Calcination of catalyst at $500\,^{\circ}C$ and $800\,^{\circ}C$, $Ce_{0.4}Zr_{0.6}O_2$ and tetragonal phase of $Ce_{0.16}Zr_{0.84}O_2$ are visible respectively. The RS results, show the oxygen vacancies/Ce^{3+} presence in different proportion in all sample.

Shin et al (2001) [17] VO_x/SiO_2 catalyst s were investigated using a packed bed reactor for selective oxidation of H_2S. The conversion of H_2S is very high values (>90%) for V_2O_5/SiO_2 at 270-350$\,^{\circ}C$.

Reddy et al (2002) [30] Characterization of $V_2O_5/CeO_2\text{-}SiO_2$ calcined at 500-800$\,^{\circ}C$. The catalyst is a very high specific surface area and the surface of SiO_2 was covered by CeO_2. At high calcination temperature, the XRD shown $CeVO_4$ peak due to the reaction between V_2O_5 and CeO_2. V^{5+} has been found at the surface when calcination temperature increased.

Kang et al (2015) [31] $CeO_2\text{-}TiO_2$ were studied for catalytic oxidation of H_2S in a vary atom ratio of Ce/Ti are 1/1 1/3, 1/5 and 3/1. The surface area of mixed-oxide $CeO_2\text{-}TiO_2$ is higher than pure cerium oxide. The highest surface area was investigated when atom ration of Ce/Ti is 1/3, decreasing of surface area occur when Ce content increased. Catalysts with Ce/Ti = 1/3 and 1/5 exhibited the highest conversion of H_2S because the uniform dispersion of metal oxides.

Table 5 Summary the research of the catalytic oxidation of H_2S to elemental sulfur.

Researcher	Study	Catalyst	Reaction condition	Result
Davydov et al. (2003) [10]	Catalytic activity of metal oxide in H_2S oxidation	MgO, CaO, La_2O_3, TiO_2 ZrO_2, V_2O_5, Cr_2O_3, MoO_3, Mn_2O_3, Fe_2O_3, CoO, NiO, CuO, ZnO, Al_2O_3, Ga_2O_3, In_2O_3, SiO_2, SnO_2, Sb_6O_{13} and Bi_2O_3	Feed concentration is 0.5 vol.% of H_2S and 0.25 vol.% of O_2 T = 250°C	V_2O_5 is the best performance for selective oxidation of H_2S to sulfur both total and selective oxidation of H_2S
Li et al (1996) [9]	Catalytic activity of vanadium-based mixed-oxide in selective oxidation of H_2S	Iron oxide Vanadium oxide Bismust oxide Magnesium oxide Molybdenum oxide V/Mo V/Bi V/Mg	Molar ratio of $H_2S:O_2$ = 1/5 T = 200 - 220°C	Vanadium oxide is the best performance and Mo, Bi and Mg significantly improve the catalytic performance more than pure vanadium oxide at any temperature

Kim et al (2006) [24]	Performance of a series of V_2O_5/TiO_2 aerogel were prepared by sol-gel method	2% V_2O_5/TiO_2 5% V_2O_5/TiO_2 10% V_2O_5/TiO_2 (aerogel) 5% V_2O_5/TiO_2 (xerogel) 5% V_2O_5/TiO_2 (impregnated)	Feed mixture composed of H_2S/O_2 = 5.0/2.5 T = 220-260°C	5% V_2O_5/TiO_2 aerogel catalyst exhibited on higher conversion of H_2S without SO_2 formation
Soriano et al (2015) [5]	Catalytic activity of V_2O_5 on porous clay heterostructure (PCH) in partial oxidation of H_2S	2% V_2O_5/PCH 4% V_2O_5/PCH 8% V_2O_5/PCH 12% V_2O_5/PCH 16% V_2O_5/PCH	Feed mixture composed of H_2S/air = 1.2/5.0 T = 180°C	The catalyst with higher V_2O_5 content are more active with higher of H_2S conversion and SO_2
Soriano et al (2009) [25]	Catalytic activity of V_2O_5 on mesoporous zirconium phosphate heterostructure (MZP) in partial oxidation of H_2S	MZP 2% V_2O_5/MZP 4% V_2O_5/MZP 8% V_2O_5/MZP 12% V_2O_5/MZP 16% V_2O_5/MZP V_2O_5	Feed mixture composed of H_2S/air = 1.2/5.0 T = 180 – 260 °C	The catalytic activity and stability increasing with the V-loading and sulfur deposit on the catalyst is flavored in catalyst with low V-loading.

Pongthawo rnsakun et al (2018) [12]	Activity of TiO_2 supported vanadium oxide for selective oxidation of H_2S	V_2O_5/anatase-43 V_2O_5/anatase-21 V_2O_5/solvo V_2O_5/P25 V_2O_5/rutile	Feed mixture composed of 300 ppm of H_2S and 150 ppm of O_2 T = 130 °C	V_2O_5/anatase-21 exhibited the best catalyst performance with 80% conversion of H_2S and low selectivity of SO_2 (<7 ppm)
Barba et al (2013) [8]	Catalytic activity of vanadium-based support on mixed oxide in partial oxidation of H_2S	CeO_2 TiO_2 $CuFe_2O_4$ V_2O_5/ CeO_2 V_2O_5/ TiO_2 V_2O_5/ $CuFe_2O_4$	Feeding 1000 ppm of H_2S, 500 ppm of O_2 T = 50 – 250 °C	V_2O_5/ CeO_2 exhibited the highest conversion of H_2S and low selectivity of SO_2.The selectivity of SO_2 decrease with reaction temperature increased.
Palma et al (2014) [11]	Catalytic activity for selective oxidation of H_2S on CeO_2 supported vanadium (V_2O_5) catalyst at varies V_2O_5 load	2.55% V_2O_5/ CeO_2 5% V_2O_5/ CeO_2 8% V_2O_5/ CeO_2 10% V_2O_5/ CeO_2 20% V_2O_5/ CeO_2	Feeding 200 ppm of H_2S,100 ppm of O_2 T = 150 – 250 °C	20 wt.% V_2O_5/CeO_2, catalyst was a good activity with 99% of sulfur selectivity and 98.7% of H_2S conversion at 150 °C

Zang et al (2013) [13]	The structural and activity of a series of vanadium supported on ceria doped with Lamponite clay catalyst for selective oxidation of H$_2$S	3% V$_2$O$_5$/Ce-Lap 5% V$_2$O$_5$/Ce-Lap 8% V$_2$O$_5$/Ce-Lap	Feeding 5000 ppm of H$_2$S, 2500 ppm of O$_2$ T = 120 – 220 $^\circ$C	5% V$_2$O$_5$/Ce-Lap catalyst presented the best catalytic activity and could be resistance the deactivation of catalyst.
Yasyerli et al (2006) [28]	Catalytic activity of Ce-V mixed oxide in partial oxidation of H$_2$S	CeO$_2$ Ce3V1 Ce2V2 Ce1V3	Molar ratio of H$_2$S/O$_2$ = 0.5 T = 200 - 300°C	Ce-V mixed oxide atomic ratio of one (Ce/V = 2/2) showed 100% H$_2$S conversion when O$_2$/H$_2$S feed ratios of 0.5 used at 250°C

2.8 Catalytic Mechanism

Although the literature widely proposed the type of mechanism for the total catalytic oxidation reaction of H$_2$S on the vanadium catalyst as Langmuir–Hinshelwood and Rideal-type or Rideal–Eley-type mechanisms. For the selective oxidation of H$_2$S reaction over supported V$_2$O$_5$ catalyst, Mars-van Krevelen or so-called redox mechanism is usually established to explain the oxidized active site on the catalyst surface oxidizes the reactant and regenerated back to the original (re-oxidized) by the oxygen in gas phase in a stepwise mechanism [10].

A stepwise mechanism for the selective oxidation of H_2S reaction over supported V_2O_5 catalyst is shown in Figure 4. First, the reaction occurs on the active site vanadium with H_2S in gas phase. H_2S adsorbed on the active site and take oxygen atom from V_2O_5 to produce the products of sulfur element and water. H_2S was oxidized to sulfur by V^{5+}. At the same time, V^{5+} was reduced to V^{4+} then oxygen vacancies occurred. Simultaneously, oxygen in the gas phase was adsorbed on the catalyst surface, V^{4+} was re-oxidized back to the initial state by reacting with oxygen in the gas phase called re-oxidation. The catalytic activity was determined based on the redox cycle of V^{5+} [12]. Shin et al. [27] rate of re-oxidation step much slower than the reduction step by H_2S so, the re-oxidation step would be as the limiting step which affect significantly to the performance of the catalyst.
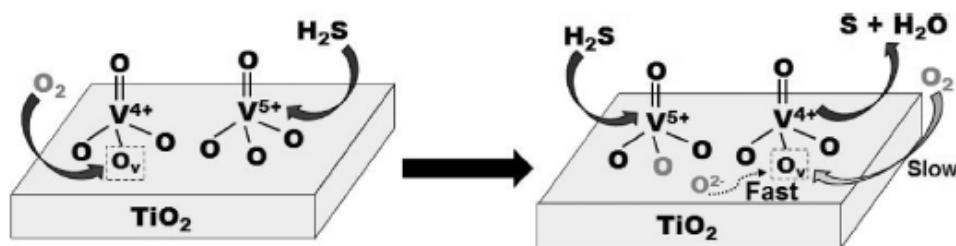
Figure 4 Proposed mechanism of H_2S selective oxidation on the supported V_2O_5 [12]

CHAPTER III

MATERIALS AND METHODS

The experiment is described in this chapter, which is divided into three parts including catalyst preparation, catalyst characterization, and H_2S oxidation reaction test.

3.1 Catalyst preparation

V_2O_5 (3 wt.%) on the CeO_2 and modified CeO_2-MO_2 mixed-oxides (M = Ti^{4+}, Si^{4+} and Zr^{4+}) support were prepared by wet impregnation.

3.1.1 Preparation of CeO_2 support

CeO_2 was prepared into two samples, The first one is commercial powder CeO_2 provide by Sigma-Aldrich and the second one was synthesized. Synthesized CeO_2 was obtained by calcination $Ce(NO_3)_3 \cdot 6H_2O$ at 500°C for 5 h in air with 10°C/min of ramp rate on temperature. The chemicals are shown in Table 6.

Table 6 The chemicals for Preparation of CeO_2-TiO_2 (1:1 molar ratio) support

Chemical	Formula	Supplier
Cerium (III) nitrate hexahydate, 99.5%	$Ce(NO_3)_3 \cdot 6H_2O$	Sigma-Aldrich
Cerium (IV) oxide, < 25 nm	CeO_2	Sigma-Aldrich

3.1.2 Preparation of CeO_2-TiO_2 (1:1 molar ratio base on oxide) support

CeO_2-TiO_2 support was synthesized by co-precipitation method. 3.5 g of cerium (III) nitrate hexahydate and 2.8 g titanium (IV) butoxide were dissolved in 30 ml of distilled water and 30 ml of ethanol respectively. The solution were mixed together. Ammonium hydroxide was added to the previous mixture solution until precipitation was complete at pH = 8 and stirred at 80°C on a heating plate for 1 h. The chemicals are shown in Table 7. After obtained hydroxide gels, the solution were washed with deionize water, dried at 110 °C overnight in oven and calcined at 500°C for 5 h in air with 10°C/min of ramp rate on temperature.

Table 7 The chemicals for Preparation of CeO_2-TiO_2 (1:1 molar ratio) support

Chemical	Formula	Supplier
Cerium (III) nitrate hexahydate, 99.5%	$Ce(NO_3)_3 \cdot 6H_2O$	Sigma-Aldrich
Titanium (IV) butoxide, 97%	$Ti(C_4H_9O)_4$	Sigma-Aldrich
Ammonium hydroxide, 28% NH_3 in water, 99.99%	NH_4OH	Sigma-Aldrich

3.1.3 Preparation of CeO_2-SiO_2 (1:1 molar ration base on oxide) support

CeO_2-SiO_2 support was synthesized by co-precipitation method. 4.7 g of ammonium cerium (IV) nitrate was dissolved in 30 ml of distilled water and mixed together with 1 ml of colloidal silica. Ammonium hydroxide was added to the previous mixture solution until precipitation was complete at pH = 8 and stirred at 80°C on a heating plate for 1 h. The chemicals are shown in Table 8. After obtained hydroxide gels, the solution were washed with deionize water, dried at 110 °C overnight in oven and calcined at 500°C for 5 h in air with 10°C/min of ramp rate on temperature.

Table 8 The chemicals for Preparation of CeO_2-SiO_2 (1:1 molar ratio) support

Chemical	Formula	Supplier
Ammonium cerium (IV) nitrate, > 99.99%	$Ce(NH_4)_2(NO_3)_6$	Sigma-Aldrich
Colloidal silica, 40 wt.% suspension in H_2O		Sigma-Aldrich
Ammonium hydroxide, 28% NH_3 in water, 99.99%	NH_4OH	Sigma-Aldrich

3.1.4 Preparation of CeO_2-ZrO_2 (1:1 molar ratio base on oxide) support

CeO_2-ZrO_2 support was synthesized by co-precipitation method. 3.2 g of cerium (III) nitrate hexahydate and 1.5 g zirconium (IV) oxynitrate hydrate were dissolved in 30 ml of distilled water separately. The solution were mixed together. Ammonium hydroxide was added to the previous mixture solution until precipitation was complete at pH = 8 and stirred at 80°C on a heating plate for 1 h. The chemicals are shown in Table 9. After obtained hydroxide gels, the solution were washed with deionize water, dried at 110 °C overnight in oven and calcined at 500°C for 5 h in air with 10°C/min of ramp rate on temperature.

Table 9 The chemicals for Preparation of CeO_2-TiO_2 (1:1 molar ratio) support

Chemical	Formula	Supplier
Cerium (III) nitrate hexahydate, 99.5%	$Ce(NO_3)_3 \cdot 6H_2O$	Sigma-Aldrich
Zirconium (IV) oxynitrate hydrate, 99%	$ZrO(NO_3)_2 \cdot 2H_2O$	Sigma-Aldrich
Ammonium hydroxide, 28% NH_3 in water, 99.99%	NH_4OH	Sigma-Aldrich

3.1.5 Preparation of 3 wt.% V_2O_5 over CeO_2 and CeO_2-MO_2 Catalyst

3 wt.% V_2O_5 over CeO_2-MO_2 was synthesized by wet impregnation method. Ammonium metavanadate was dissolved in 1 M of oxalic acid solution and adding support into the solution. The chemicals are shown in Table 10. The solution was stirred at 80°C on a heating plate until completing in evaporating, dried at 110 °C overnight in oven and calcined at 500°C for 5 h in air with 10°C/min of ramp rate on temperature.

Table 10 The chemicals for Preparation of 3 wt.% V_2O_5 over CeO_2-MO_2 Catalyst

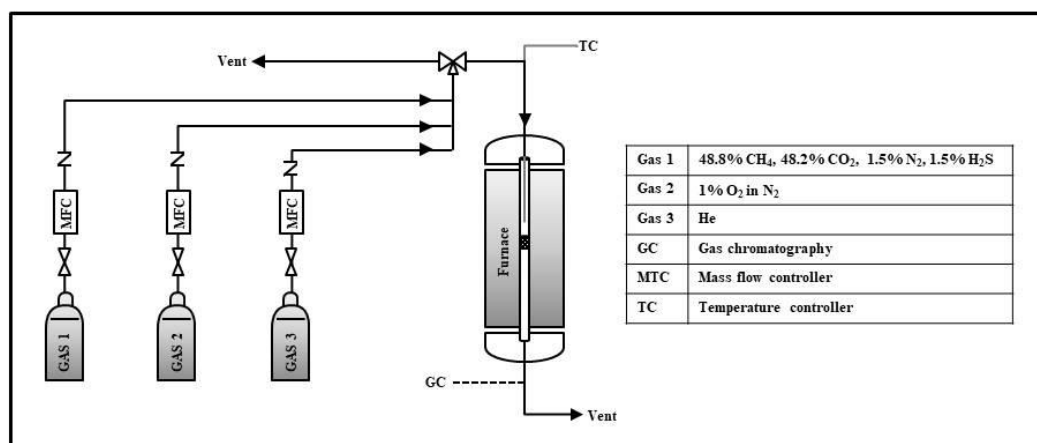| Chemical	Formula	Supplier
Ammonium metavanadate, 99.99%	NH_4VO_3	Sigma-Aldrich
Cerium (IV) oxide, < 25 nm	CeO_2	Sigma-Aldrich
Mixed-oxide support from 4.1.1-4.1.3	CeO_2-MO_2	-

3.2 Reaction test in H_2S oxidation

Figure 5 Flow diagram of H_2S oxidation reaction system.

0.03 g of catalysts were packed into the glass fixed bed reactor which the inner diameter is 9 mm, supported the catalyst with 0.15 g of quartz wool. Before the reaction test, the catalyst was pretreat with 50 ml/min of Helium at 200 $^\circ$C for 1 h. The activity test for selective oxidation of H_2S were carried out in temperature of 130 $^\circ$C and atmospheric pressure for 3 h with gaseous mixture feed containing of 400 ppm of H_2S, 200 ppm of O_2, 1.3% of CH_4, 1.3% of CO_2, and 2% of N_2 balanced with helium. The total flow rate of feed is 320 ml/min was mixed from gas 1, gas 2 and gas 3 are shown in the Table 11. Sulfur dioxide (SO_2) and hydrogen sulfide (H_2S), was analyzed by a gas chromatograph (GC-2014) containing Porapak QS column. Methane (CH_4) and carbon dioxide (CO_2) were analyzed by a gas chromatograph (GC-8A) containing Porapak Q column. A flow diagram of reaction system are shown in Figure 5. Operating condition of gas chromatography are shown in Table 12. The conversion of H_2S were calculated by following equation:

$$x\% \ H_2S = (H_2S \ reacted/ \ H_2S \ fed) \times 100 \qquad \text{---------------------- (14)}$$

Table 11 Gas materials used in the reaction test.

Gas NO.	Gas materials	Supplier
Gas 1	Methane 48.8%, Carbon dioxide 48.2%, Nitrogen 1.5%, and Hydrogen sulfide 1.5%	Linde
Gas 2	1% Oxygen in Nitrogen	Linde
Gas 3	Helium Ultra High Purity (Purity 99.999%)	BIG

Table 12 Operating condition of gas chromatographs.

Gas Chromatograph	GC-2014	GC-8A
Detector	FPD	TC
Column	Porapak QS	Polarpak Q
Carrier gas	Helium	Helium
Injection temperature	120	100
Column temperature (Initial)	140	70
Column temperature (Final)	236	70
Detector temperature	250	100
Analyzer gas	H_2S and SO_2	CH_4 and CO_2
Retention time	23	10

3.3 Catalyst characterization

3.2.1 X-ray diffraction (XRD)

The X-ray diffraction (XRD) patterns were investigated by a SIEMENS D5000 X-ray diffractometer with radiation of CuKα in scanning rate of 0.5 sec/step ($2\theta = 20°$ to $80°$). The crystallite size was calculated using the Scherrer's equation and α-alumina as the external standard.

3.2.2 Raman spectroscopy

Raman spectra used to analyzed the functional group of catalysts. The spectra were obtained on a spectrometer (DILORXY) with a CCD detector (liquid nitrogen cooled) with an Ar^+ laser, emission line at 514.5 nm. Analyze in Raman shift of 100-1300 cm^{-1} are accurate within 2 cm^{-1}. The power incident beam was 3 mW. The analyzed spot was 1 μm.

3.2.3 N_2-physisorption

The BET surface area (m^2/g), average pore size diameters (nm), and pore volume (cm^3/g) of catalyst were investigated by using N_2 physisorption technique on a Micromeritics ASAP 2020 automated system.

3.2.4 Inductively coupled plasma-optical emission spectrometry (ICP-OES)

The actual percentages of V_2O_5 loading of the catalysts were measured by inductively coupled plasma-optical emission spectrometry (ICP-OES), using an Iris advantage Thermo Jarrel Ash devide. The principle of ICP is the instrument to analyze the number of elements in samples that were completely degraded to solution. Preparation of sample analysis by 0.01 g of catalyst was dissolve in 5 ml of sulfuric acid (98%) and then dilute with 100 ml of deionized water.

3.2.5 Scanning electron microscopy with energy dispersive X-ray spectroscopy (SEM-EDX)

The morphology of catalysts and elemental distribution on the surface of catalysts were analyzed by Scanning Electron Microscopy with Energy Dispersive X-Ray Analysis (SEM-EDX) using Link Isis series 300 program SEM (JEOL model JSM-5800LV).

3.2.6 Fourier transform infrared spectroscopy (FT-IR)

The functional group of catalysts were analyzed by the Fourier transform infrared spectroscopy (FT-IR) that can analyze in the range of 400-4000 cm^{-1}. The resolution was 4 and a number of scan was 200.

3.2.7 Oxygen-Temperature programmed desorption (O$_2$-TPD)

Temperature programmed desorption of oxygen (O$_2$-TPD) technique was used to analyze the amount of oxygen (O$_2$) in the catalyst. 0.1 g of catalyst was packed in quartz reactor supported by quartz wool. In order to removal moisture in the catalyst, the catalyst was pre-heated with helium at 350 $^{\circ}$C for 1 h and then cooled down to the room temperature. After that, 50 ml/min of the of 1% of O$_2$ in He was fed into the reactor for 1 h at room temperature. Then, purge the residual oxygen by He for 1.5 h. Finally, Temperature programmed desorption of oxygen was increased from room temperature to 800 $^{\circ}$C (ramp rate of 10 $^{\circ}$C/min) The effluent of oxygen concentration was continuously recorded by using a thermal conductivity detector.

3.2.8 X-ray photoelectron spectroscopy (XPS)

The surface properties such as electronic state, chemical state, and atomic elemental concentrations were determined by the XPS on a Kratos Amicus X-ray photoelectron spectrometer with Mg Kα X-ray source. The internal standard of XPS spectra of C 1s line at binding energy was 285.0 eV.

CHAPTER IV
RESULTS AND DISCUSSION

The characteristics and catalytic activity of V_2O_5 dispersed on pure CeO_2 and CeO_2-MO_2 mixed oxide supports prepared with different molar ratios between CeO_2 and MO_2 in the selective oxidation of H_2S to sulfur element were reported and discussed in this chapter. The properties and characteristics of catalysts were analyzed by X-ray diffraction (XRD), Raman spectroscopy, N_2-physisorption, inductively coupled plasma-optical emission spectrometry (ICP-OES), scanning electron microscopy with energy dispersive X-ray spectroscopy (SEM-EDX), Fourier transformed Infrared spectroscopy (FT-IR), X-ray photoelectron spectroscopy (XPS), and oxygen-temperature programmed desorption (O_2-TPD. In the last part, the catalytic performed in H_2S oxidation at 130 $^\circ$C and atmospheric pressure were discussed.

4.1 X-ray diffraction (XRD)

The X-ray diffraction (Figure 6) was used to investigate the structure of V_2O_5 supported on different supports. The X-ray diffraction peak corresponding to cerium oxide were evidenced at 2 theta ~ 28.6 $^\circ$, 33.1 $^\circ$, 47.5 $^\circ$, and 56.3 $^\circ$ [31, 32]. The peaks at 2 theta ~ 28.6 $^\circ$, 33.2 $^\circ$, 47.5 $^\circ$, and 56.3 $^\circ$ suggesting CeO_2 were observed for all catalysts, whereas the diffraction peaks corresponding to V_2O_5 were not detected, suggesting that they were highly dispersed on the support at low 3 wt.% loading. According to the literature [33], the XRD peak of V_2O_5 supported on ceria appeared when V_2O_5 was increased to more than 20 wt.%. The X-ray diffraction peaks of cerium vanadate which could be obtained from the reaction between CeO_2 and V_2O_5 due to high calcination temperature (> 500 $^\circ$C) and high V_2O_5 loading (> 20% wt.%) according to the following reaction were also not detected [11]:

$$CeO_2(s) \ + \ 0.5V_2O_5(s) \ \longrightarrow \ CeVO_4(s) \ + \ 0.5O_2(g) \ \text{----------------} \ (15)$$

For the case of mixed oxide support catalysts (Figure 7-8), no diffraction peak of SiO_2 were detected as it is known to be an amorphous [30]. In case of V_2O_5/CeO_2-TiO_2, a diffraction patterns of the ceria along with low intensity TiO_2 anatase phase peak were observed. The anatase phase TiO_2 with high crystallinity can be observed at 2 theta ~ 25°, 37°, and 53° [34]. Preuss et al. [35] reported Ce-Ti-O oxides specifically Ce_2TiO_5, $Ce_2Ti_2O_7$ and $Ce_4Ti_9O_{24}$ by heating the mixtures of solida containing Ce and Ti at high temperature of 1250° C. However, the crystalline phase as mentioned could not be observed in the present study due to lower calcination temperature of 500° C. Lin et al. [36] suggested the Ti^{4+} enter the CeO_2 lattice at the interface to form octahedral site because titanium is locked by 8 coordinated oxygen atoms as surrounding cerium [36, 37]. For V_2O_5/CeO_2-ZrO_2, in addition to the CeO_2 X-ray diffraction peaks, the X-ray diffraction of another cubic fluorite-type in composition of $Ce_{0.4}Zr_{0.6}O_2$ was detected at 2 theta ~ 29.8°, 34.8°, 49.6° and 58.3° [38].
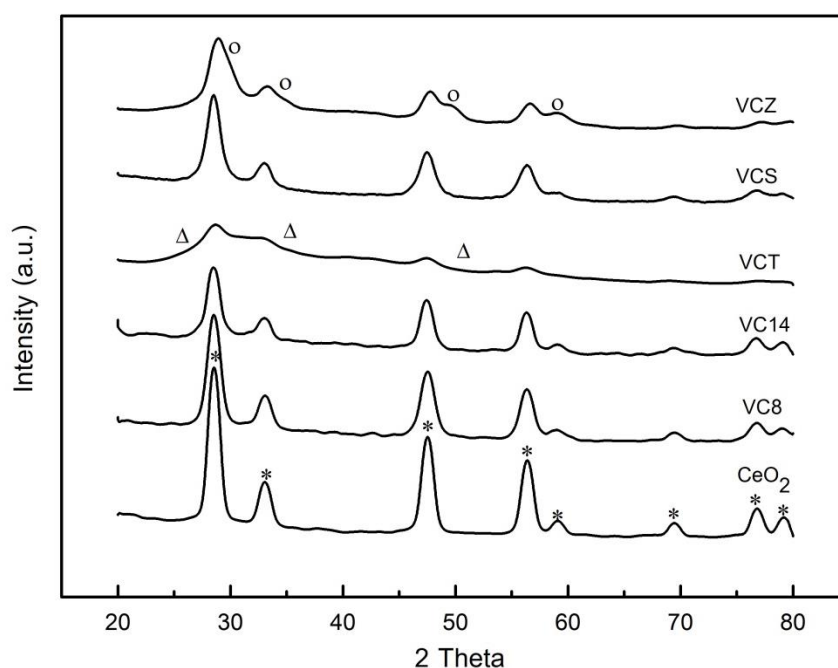
Figure 6 X-ray diffraction patterns of V_2O_5/CeO_2-14 (VC14), V_2O_5/CeO_2-8 (VC8), V_2O_5/CeO_2-TiO_2 (VCT), V_2O_5/CeO_2-SiO_2 (VCS) and V_2O_5/CeO_2-ZiO_2 (VCZ) catalyst: (*) line due to CeO_2; (Δ) line due to TiO_2 anatase; (o) line due to $Ce_{0.4}Zr_{0.6}O_2$.
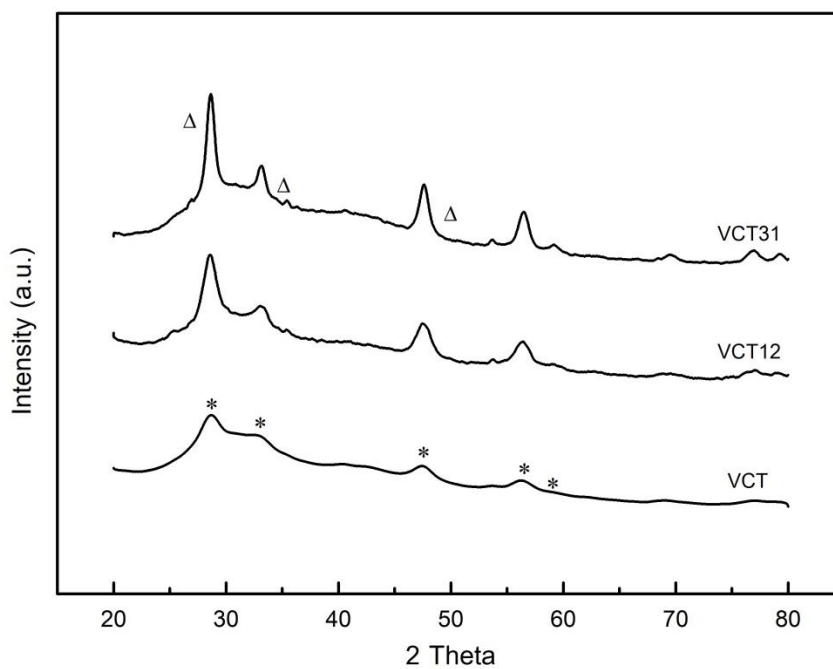
Figure 7 X-ray diffraction patterns of V_2O_5/CeO_2-TiO_2 (VCT) with vary molar ratio base oxide (CeO_2:TiO_2) catalyst: (*) line due to CeO_2; (Δ) line due to TiO_2 anatase.
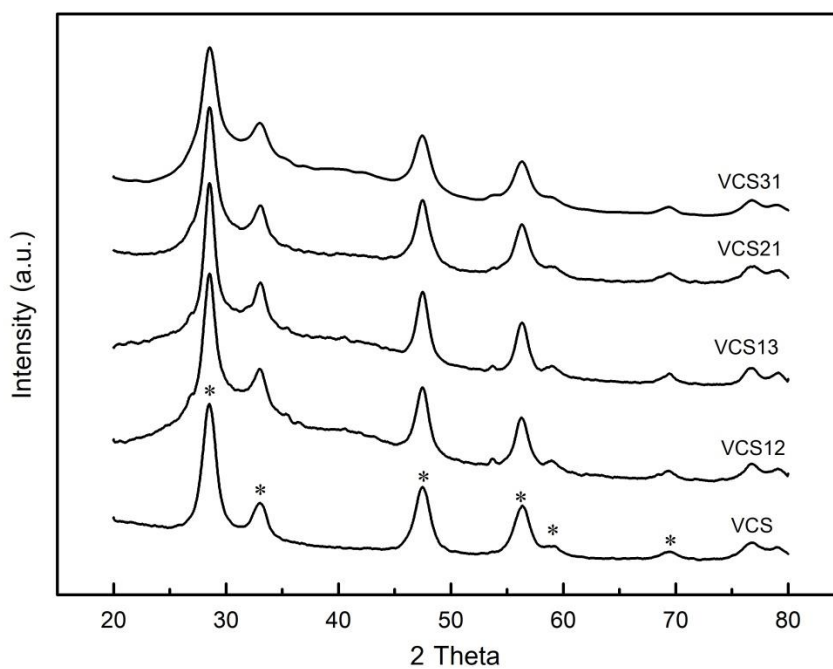

Figure 8 X-ray diffraction patterns of V_2O_5/CeO_2-SiO_2 (VCS) with vary molar ratio base oxide (CeO_2:SiO_2) catalyst: (*) line due to CeO_2.

4.2 Raman spectroscopy

High specific surface area V_2O_5/CeO_2-SiO_2 and low specific surface area V_2O_5/CeO_2-TiO_2 catalysts were selected for the investigation of the dispersion of V_2O_5 on the support in comparison to the V_2O_5/CeO_2-8 by Raman spectroscopy technique. Figure 9 showed raman spectra of ceria at 462 cm^{-1}. No peaks corresponding to the crystalline of V_2O_5 were observed for all the samples (Raman spectra at 995, 702, 527, 404 and 284 cm^{-1}), in agreement with the results from XRD that all the catalysts exhibited good dispersion of the vanadium species on the supports. [29, 39]
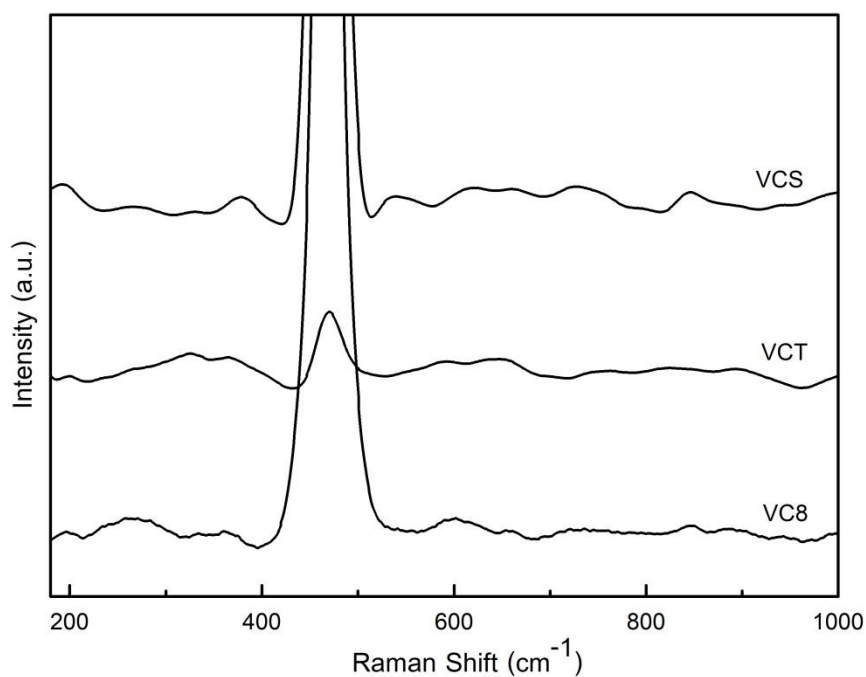

Figure 9 Raman spectroscopy of V_2O_5/CeO_2-8 (VC8), V_2O_5/CeO_2-TiO_2 (VCT) and V_2O_5/CeO_2-SiO_2 (VCS) catalyst.

4.3 N_2-physisorption

The BET surface area (m^2/g), pore volume (cm^3/g), and average pore diameter (nm) of the catalysts are given in the Table 13. Clogging of the catalyst pores from V_2O_5 species resulted in low distribution on the surface. V_2O_5/CeO_2-SiO_2 had the highest specific surface (144.5 m^2/g) and was higher than pure supported ceria V_2O_5/CeO_2-8 and V_2O_5/CeO_2-14 (56.7 and 49.1 m^2/g, respectively). The high specific surface area of V_2O_5/CeO_2-SiO_2 corresponded to the highest amount of pore volume (0.28 cm^3/g). On the other hand, V_2O_5/CeO_2-TiO_2 had lowest specific surface area and the lowest amount of pore volume (0.04 cm^3/g). The average crystal size of CeO_2 was calculated from the FWHM (full width at half maximum) of XRD peak corresponding to crystalline of CeO_2 at 2 theta $\sim$ 28.6° in Figure 6-8 using the Scherrer's equation . Smaller crystallite size of CeO_2 in the range of 3-6 nm was found on all the mixed-oxide supported catalysts. The crystallite size decreased in the following order: V_2O_5/CeO_2-14 (14 nm) > V_2O_5/CeO_2-8 (8 nm) > V_2O_5/CeO_2-SiO_2 (5 nm) > V_2O_5/CeO_2-TiO_2 = V_2O_5/CeO_2-TiO_2 (3 nm).

Table 13 Vanadium composition (wt.%) and physical properties of 3 wt.% V_2O_5/CeO_2-MO_2 catalyst

Catalyst	N_2 Physisorption			Crystallize size of CeO_2 (nm)[a]
	SA (m^2/g)	Pore volume (cm^3/g)	Average pore diameter (nm)	
3%V_2O_5/CeO_2-8 (VC8)	56.7	0.18	11.9	8
3%V_2O_5/CeO_2-14 (VC14)	49.1	0.10	7.6	14
3%V_2O_5/CeO_2-TiO_2 (VCT)	27.0	0.04	6.0	3
3%V_2O_5/CeO_2-SiO_2 (VCS)	144.5	0.28	7.8	5
3%V_2O_5/CeO_2-ZrO_2 (VCZ)	69.8	0.09	4.7	3

[a] Crystallite size was calculated from the Scherrer's equation

From the above characterization results from N_2 physisioption and XRD, small crystallite size of CeO_2 and high specific surface area were obtained after SiO_2 was doped to the V_2O_5/CeO_2 with molar ratio 1:1 based on mixed-oxide support so, the ratio of CeO_2-SiO_2 was further varied in different ratios at 1:2, 1:3, 2:1 and 3:1 to investigate the physical properties and performances of CeO_2-SiO_2 supported catalysts. From Table 14, it was found that increasing SiO_2 molar ratio resulted in the increased specific surface area, and vice versa for increasing CeO_2 molar ratio. In the case of V_2O_5/CeO_2-TiO_2 with molar ratio 1:1, 1:2 and 2:1, the specific surface area were not much changed between 19.8-21.4 m^2/g and were found to be less than the pure supported ceria (V_2O_5/CeO_2-8 and V_2O_5/CeO_2-14). The crystallite size of CeO_2 on all the mixed-oxide supported catalyst were also in the range of 3-6 nm.

Table 14 Vanadium composition (wt.%) and physical properties of 3 wt.% V_2O_5/CeO_2-MO_2 with vary molar ratio base metal oxide between CeO_2 and MO_2 catalyst.

Catalyst	N_2 Physisorption SA[a] (m^2/g)	Crystallize size of CeO_2 (nm)[b]
VC8	46.3	8
VC14	40.2	14
VCT	19.8	3
VCT12	20.5	3
VCT21	21.4	6
VCS	107.6	5
VCS12	136.6	4
VCS13	145.2	5
VCS21	99.7	5
VCS31	79.3	4
VCZ	50.1	3

[a] SA were characterize from N_2 physisorption on monolayer

[b] Crystallite size was calculated from the Scherrer's equation

4.4 Inductively coupled plasma-optical emission spectrometry (ICP-OES) and Scanning electron microscopy with energy dispersive X-ray spectroscopy (SEM-EDX)

The actual metal loading amounts on the mixed metal oxide supports as determined by the ICP-OES shown in Table 15 were close to the design amount at 3 wt.% V_2O_5 loading amount. The analysis results from EDX showed the composition of element, V_2O_5/CeO_2-SiO_2 had the highest vanadium distribution on the surface of support compared to the other catalyst .

Table 15 Vanadium composition (wt.%) of 3 wt.% V_2O_5/CeO_2-MO_2 with vary molar ratio base metal oxide between CeO_2 and MO_2 catalyst.

Catalyst	EDX (wt.%)				ICP^b
	O	V	Ce	M^a	V (wt.%)
VC8	15.3	0.8	83.9	-	2.7
VC14	15.0	0.6	84.4	-	3.3
VCT	24.5	0.8	56.2	18.3	3.1
VCT12	30.4	1.8	43.0	24.8	2.8
VCT21	23.2	3.4	44.5	15.9	3.0
VCS	23.9	1.7	55.3	19.1	2.9
VCS12	40.7	6.4	15.5	37.5	2.8
VCS13	20.7	2.0	70.6	6.6	3.2
VCS21	25.2	3.8	65.5	5.5	3.1
VCS31	20.4	2.2	56.3	5.9	2.7
VCZ	20.3	0.9	40.3	38.5	3.2

[a] M = Mixed-oxide for VCT (M = Ti), VCS (M = Si) and VCZ (M = Zr)

[b] wt.% of V_2O_5

4.5 Fourier transforms infrared spectroscopy (FT-IR)

The Fourier transforms infrared spectroscopy (FTIR) spectra of the catalysts are shown in Figure 10-12. The Ce-O stretching mode was seen between at 500-700 cm^{-1} [40]. According to the spectra, the presence of CeO_2 particles were confirmed [40, 41]. The bands were attributed to the bending vibration of adsorbed water appearing at around 1660 cm^{-1}. For the –OH groups, the broad bands are shown at 3200-3600 cm^{-1} [6, 42]. To confirm the formation of V_2O_5, overtone of V=O absorption bands mod was assigned at 1900-2100 cm^{-1} [39]. The band at 1083 cm^{-1} which was clearly observed, was attributed to the Si-O-Si stretching [8]. In case of VCT, the peak was seen around between at 600-800 cm^{-1} related to the O-Ti-O bonding in TiO_2 anatase phase [43, 44]. The attributed to the vibration of ZrO_3^{2-}, the region between at 497-502 cm^{-1} were observed [45, 46].
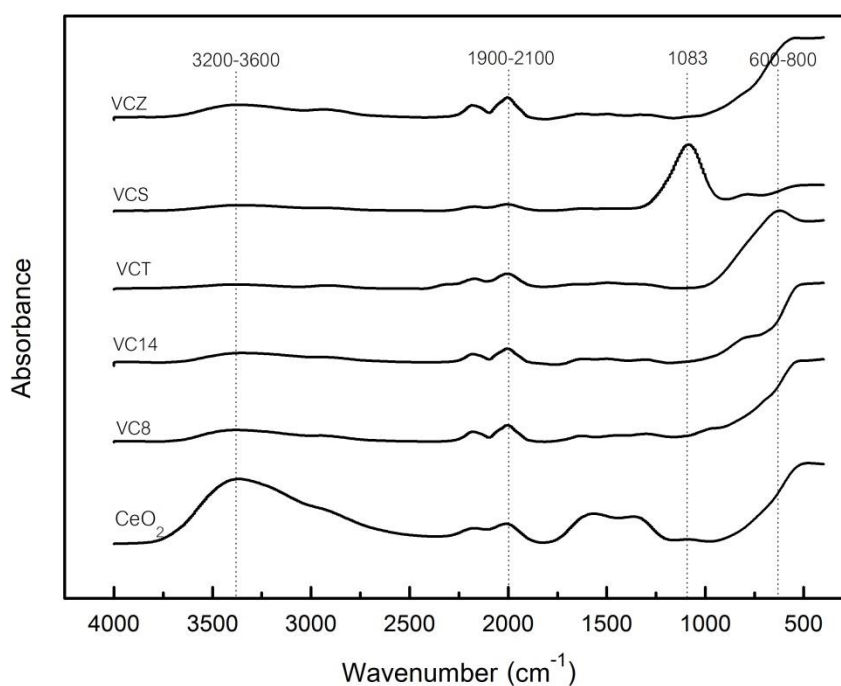

Figure 10 FTIR sprctra of V_2O_5/CeO_2-14 (VC14), V_2O_5/CeO_2-8 (VC8), V_2O_5/CeO_2-TiO_2 (VCT), V_2O_5/CeO_2-SiO_2 (VCS) and V_2O_5/CeO_2-ZiO_2 (VCZ) catalyst.
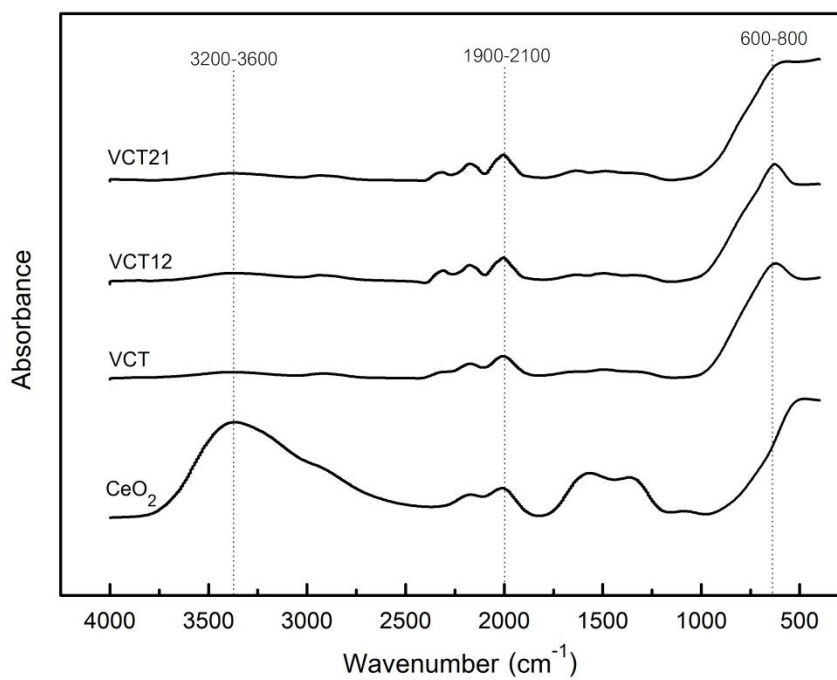
Figure 11 FTIR sprctra of V_2O_5/CeO_2-TiO_2 (VCT) with vary molar ratio base oxide

(CeO_2:TiO_2)
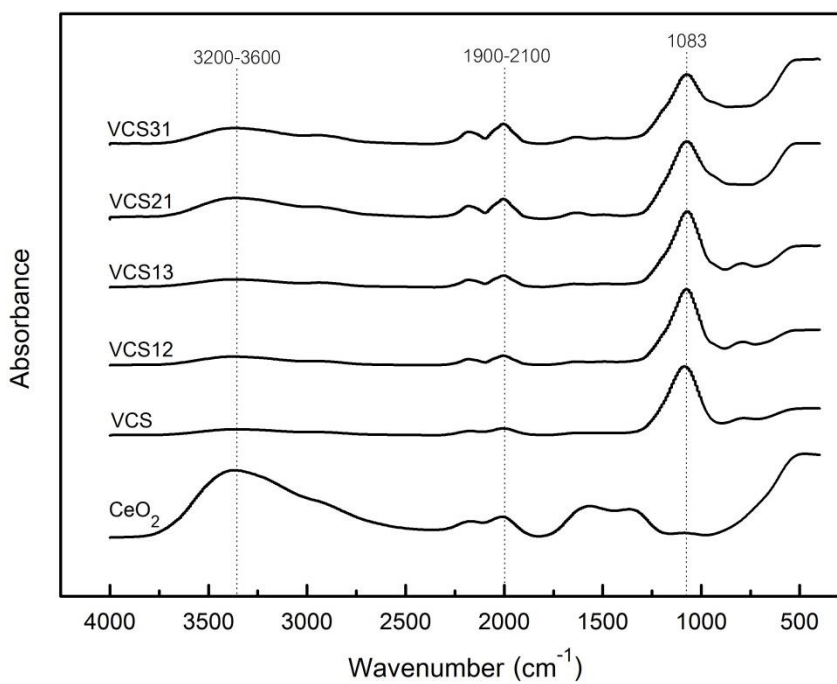
Figure 12 FTIR sprctra of V_2O_5/CeO_2-SiO_2 (VCS) with vary molar ratio base oxide

(CeO_2:SiO_2)

4.6 Oxygen-Temperature programmed desorption (O_2-TPD)

The oxygen-temperature programmed desorption (O_2-TPD) analysis was carried out in order to investigate the ability to adsorb and desorb molecules of oxygen on the catalyst surface, the analysis results are shown in Figure 15-17. The first peak at low temperature less than 300 $^\circ$C represent to the physically adsorbed oxygen (O_2^-) or weakly chemisorbed oxygen. The peak area consistent with the specific area of catalyst. The high peak area of V_2O_5/CeO_2-SiO_2 explained the high specific surface area of catalyst. The second desorption peak appeared at 300-700 $^\circ$C corresponding to strongly chemically adsorbed oxygen (O_2^{2-}/O^-) on the oxygen vacancies. The desorption peak of chemically adsorbed oxygen was observed at lower temperature on V_2O_5/CeO_2-SiO_2 suggesting that the desorption of chemically adsorbed oxygen on the oxygen vacancies for V_2O_5/CeO_2-SiO_2 was easier than the others catalyst. It is indicated that the capability of adsorption, mobility and desorption of oxygen (O_2^{2-}/O^-) on oxygen vacancies was easier which resulted in the faster re-oxidation step of V^{4+} to V^{5+} than the others catalyst. In the case of V_2O_5/CeO_2-TiO_2, a sharp second peak around temperature of 200-700 $^\circ$C corresponded to the chemically adsorbed oxygen on the oxygen vacancies but the peak shifted to high temperature so, the re-oxidation step of reaction must be slower than V_2O_5/CeO_2-SiO_2. Henrik Hogh et al. [47] also suggested that the largest peak of chemically adsorbed oxygen on the oxygen vacancies on V_2O_5/CeO_2-TiO_2 due to the oxygen vacancies on the support titania. The unpaired of electron occur when oxygen atom of titania was removed to form oxygen vacancies while V_2O_5/TiO_2 synthesized, reduce Ti^{4+} to Ti^{3+}. The electron will react to the V_2O_5 to form VO^{3-} and VO^{2-}. The desorption peaks, which were observed at higher temperature (700-800 $^\circ$C) due to desorption of lattice oxygen (O^{2-}). Obviously, the oxygen vacancy promote the O_2 dissociative adsorption to formation the oxygen ion (O^{2-}) which could re-oxidize the partially active phase of V_2O_{5-x} component [31, 48, 49].
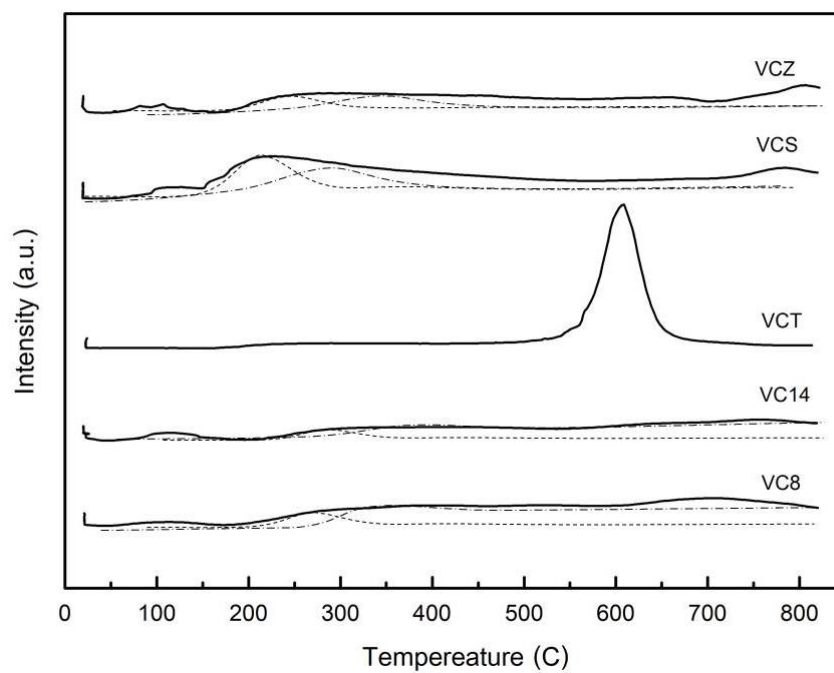
Figure 13 O_2-TPD profile of V_2O_5/CeO_2-14 (VC14), V_2O_5/CeO_2-8 (VC8), V_2O_5/CeO_2-TiO_2 (VCT), V_2O_5/CeO_2-SiO_2 (VCS) and V_2O_5/CeO_2-ZiO_2 (VCZ) catalyst:
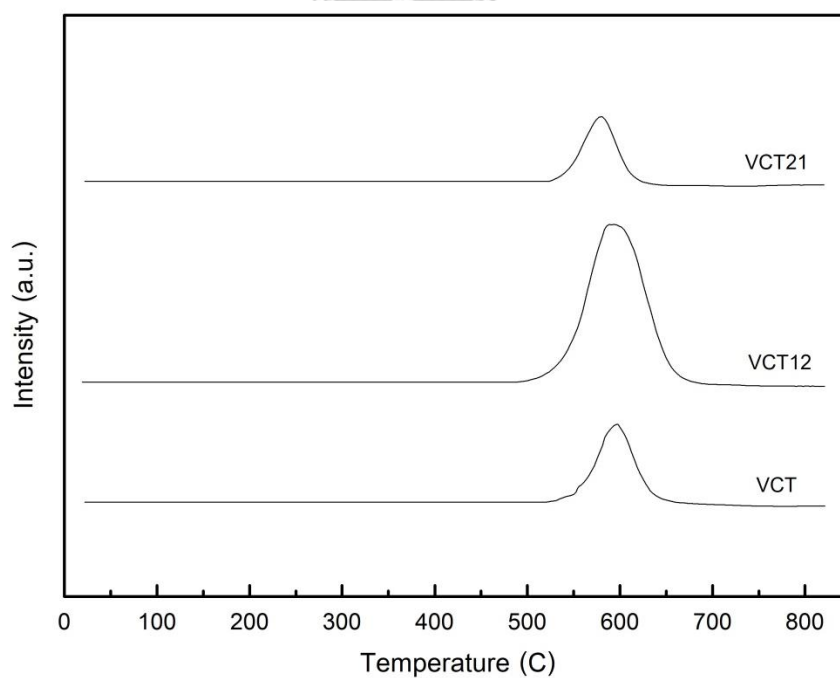

Figure 14 O_2-TPD profile of V_2O_5/CeO_2-TiO_2 (VCT) with vary molar ratio base oxide (CeO_2:TiO_2)
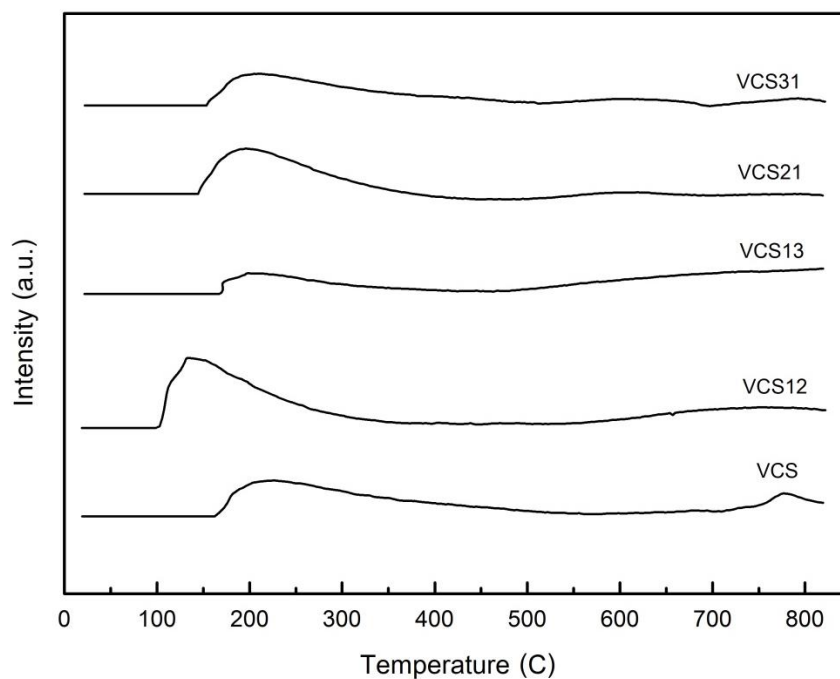
Figure 15 O_2-TPD profile of V_2O_5/CeO_2-SiO_2 (VCS) with vary molar ratio base oxide
(CeO_2:SiO_2)

4.7 X-ray photoelectron spectroscopy (XPS)

The chemical state of Ce 3d and O 1s and surface composition were investigated by using XPS technique. The XPS spectra of Ce 3d of catalysts are shown in Figure 16, the peaks labeled p and q are related to spin-orbital state of $3d_{2/5}$ and $3d_{2/3}$, respectively. Additional, the labeled p1 and q1 correspond to Ce^{3+} whereas the peaks label p, p2, p3, q, q2 and q3 represent to Ce^{4+}. The partial existence of Ce^{3+} was determined by XPS analysis. The area percentage of Ce^{3+} is determined to be VC8 (40%) > VC14 ≈ VCT ≈ VCS ≈ VCZ (19-22%) > VCS12 (12%). As is known Ce^{3+} can result in a charge imbalance, oxygen vacancies occur on the surface of catalyst are favorable for the formation of chemically adsorbed oxygen on the oxygen vacancies, which has been reported to be the most active oxygen directly affect to performance of catalyst in the oxidation reaction [32].
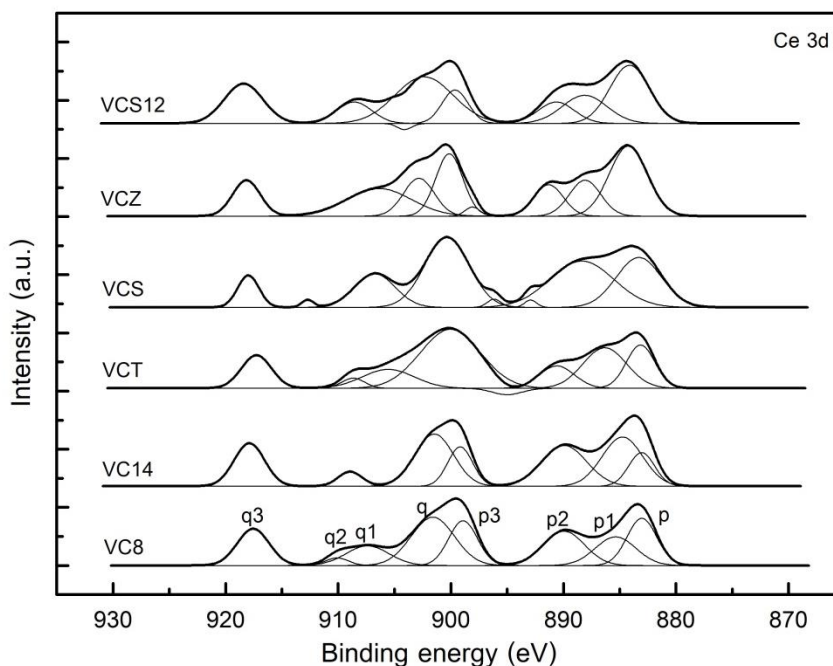
Figure 16 XPS Ce 3d spectra of V_2O_5/CeO_2-14 (VC14), V_2O_5/CeO_2-8 (VC8), V_2O_5/CeO_2-TiO_2 (VCT), V_2O_5/CeO_2-SiO_2 (VCS), V_2O_5/CeO_2-ZiO_2 (VCZ) and V_2O_5/CeO_2-SiO_2 1:2 (VCS12) catalyst.

The XPS spectra of O 1s were deconvoluted into 3 peaks representing 3 types of oxygen species as shown in Figure 17. The binding energy values of O 1s reported around 530 eV was attributed to the lattice oxygen species (O_l) of V_2O_5 and CeO_2 while the binding energy values of O 1s reported around 531.5 eV was represented to the surface oxygen (O_S) although the binding energy values of O 1s reported around 533 eV was accordance with the adsorbed molecular water (O_W). The surface oxygen related to the chemically adsorbed oxygen on the oxygen vacancies, which has been reported to be the most active oxygen directly affect to performance of catalyst in the oxidation reaction. From Table 4.4, the ratios of $O_S/(O_l+O_S)$ were found to be in the following order: VCT > VCZ > VC8 > VC14. Liu et at. [50] suggested the O 1s peak around 533 eV of V_2O_5/CeO_2-SiO_2 correspond to oxygen in SiO_2, ensure the ability to adsorb water of silica

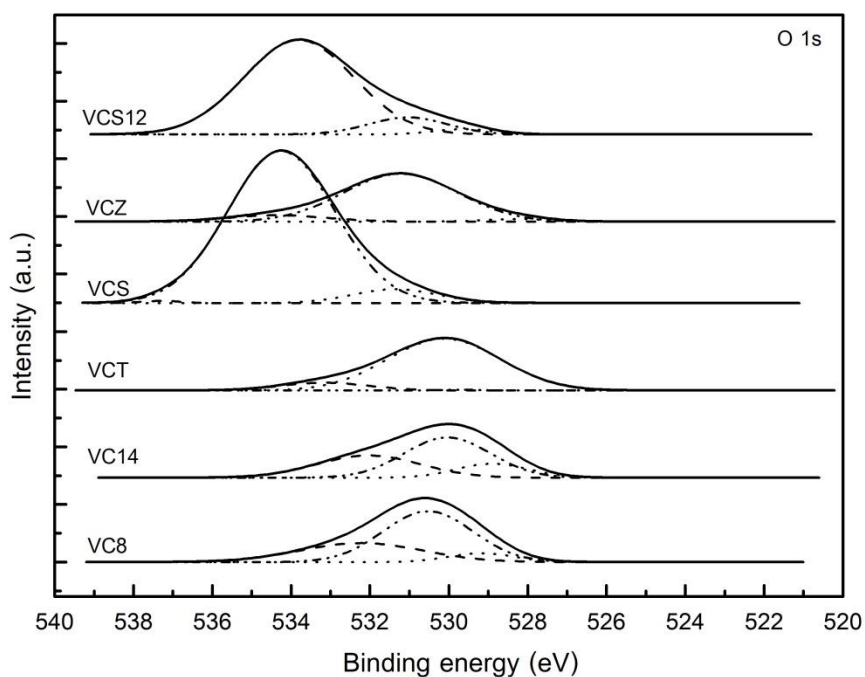encourage to larger peak of adsorbed molecular water (O_W) observed and complicate the other peaks.

Figure 17 XPS O 1s spectra of V_2O_5/CeO_2-14 (VC14), V_2O_5/CeO_2-8 (VC8), V_2O_5/CeO_2-TiO_2 (VCT), V_2O_5/CeO_2-SiO_2 (VCS), V_2O_5/CeO_2-ZiO_2 (VCZ) and V_2O_5/CeO_2-SiO_2 1:2 (VCS12) catalyst.

The XPS spectra of V 2p were fitted and deconvoluted into 2 peaks indicating of V^{5+} and V^{4+} species in form of V_2O_5 and V_2O_4, respectively (Figure 18). According to the literature, the binding energy of vanadium ions in form of vanadium oxide for instance V_2O_5, V_2O_4 and V_2O_3 reported around 517.2-517.7 eV, 516.2-516.6 and 515.2-515.9 eV. Nevertheless, the biding energy of V 2p in this study were slightly shifted higher due to decreasing of electron around V atom as Chi et al. [20] reported, due probably to the intimate contact of the two metal oxides (active site and support) caused the decrease in electron density of V and Ce resulting in higher binding energy of V 2p on the V_2O_5/CeO_2 catalyst. However, the partial existence of V^{4+} was determined by XPS

analysis, and the area percentage of $V^{4+}/(V^{4+}+V^{5+})$ is found to be VC8 > VC14. For the other catalysts, the chemical state of V species could not be detected by XPS. The lower valence state of vanadium ion may be formed, which related to interaction between vanadium oxide and support [21]. Therefore, V^{4+} could be more oxygen vacancies for improving the electron transfer result to strong redox capability.
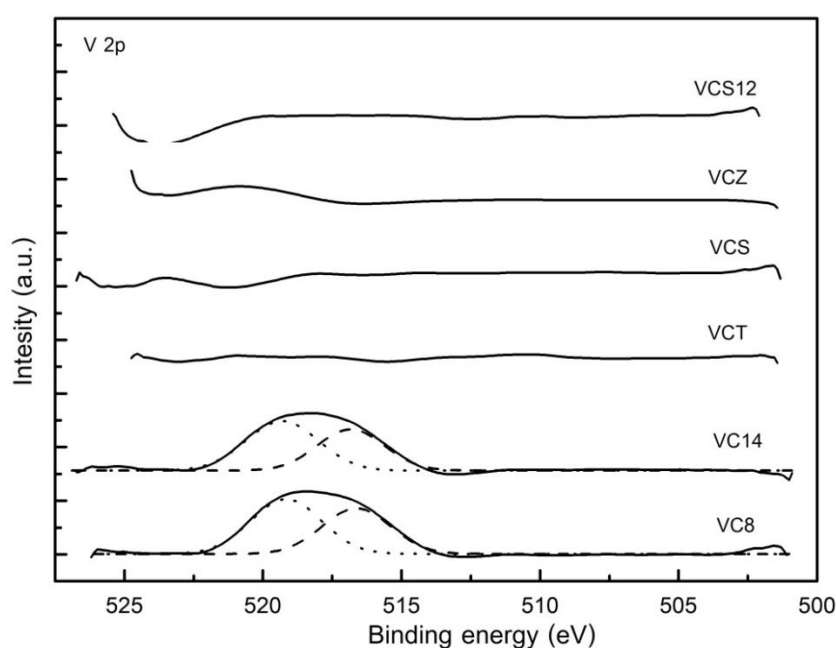

Figure 18 XPS V 2p spectra of V_2O_5/CeO_2-14 (VC14), V_2O_5/CeO_2-8 (VC8), V_2O_5/CeO_2-TiO_2 (VCT), V_2O_5/CeO_2-SiO_2 (VCS), V_2O_5/CeO_2-ZiO_2 (VCZ) and V_2O_5/CeO_2-SiO_2 1:2 (VCS12) catalyst.

Table 16 The ratio of surface atomic concentration of Ce, O and V species of catalyst.

| Catalyst	$Ce^{3+}/(Ce^{3+}+Ce^{4+})$	$O_S/(O_S+O_l)$	$V^{4+}/(V^{4+}+V^{5+})$
VC8	0.21	0.89	0.45
VC14	0.21	0.77	0.43
VCT	0.19	0.97	-
VCS	0.40	n.d.	-
VCZ	0.22	0.96	-
VCS12	0.12	n.d.	-

n.d. = not determined

4.8 Catalytic test in the selective oxidation of H_2S to sulfur

The catalytic tests in the selective oxidation of H_2S to elemental sulfur were conducted in order to investigate the performances of the prepared V_2O_5 on different mixed metal oxides at temperature of 130 $^\circ$C. By plotting the conversion-time profiles in Figure 18, it can be seen that the V_2O_5/CeO_2-SiO_2 with the highest specific surface area of 149 m^2/g exhibited the highest conversion of H_2S at ∼73% during the 3 h reaction time. The V_2O_5/CeO_2-8, V_2O_5/CeO_2-TiO_2, V_2O_5/CeO_2 -14 and V_2O_5/CeO_2-ZrO_2 exhibited 66%, 64%, 61% and 57% H_2S conversion, respectively.

The nature of support plays an important role in determination the properties of catalyst, the supported vanadium interaction affects redox properties and dispersion of active site on the support. Previous report showed that CeO_2 has the ability to capture, store and transfer surface oxygen species which exhibits exceptional redox properties so, presumable supplies active oxygen to V_2O_5 that are reduced during the reaction [34, 51]. In the present study, different metal oxides (TiO_2, SiO_2 and ZrO_2) were doped to modify the catalysts. The smaller CeO_2 crystallite size suggested the subsistence of a strong interaction between CeO_2 support and mixed-oxide support resulting in the improved performances of catalyst. The highest H_2S conversion on the V_2O_5/CeO_2-SiO_2 catalysts was correlated to the highest specific surface area, the smallest CeO_2 crystallite size, and the lowest desorption temperature for adsorption-desorption temperature of oxygen. In the same trend, Kugai et al. [52] reported the smaller crystallite size of ceria after Rh were doped result to highest ethanol conversion in oxidation of ethanol reaction. Kundakovic et al. [53] reported the smaller crystallite size of ceria accommodated the formation of highly reducible O_2 and increase activity of methane oxidation. The effect of crystallite size to the activity of catalyst can observed from the experiments using pure CeO_2, the results showed higher H_2S conversion on V_2O_5/CeO_2-8 (crystallite size = 8 nm) than on V_2O_5/CeO_2-14 (crystallite size = 14 nm).

Considering the V_2O_5/CeO_2-TiO_2 and V_2O_5/CeO_2-ZrO_2, the conversion of H_2S were lower than V_2O_5/CeO_2-SiO_2 although the crystallite sizes of CeO_2 were quite similar but the specific surface area of the V_2O_5/CeO_2-TiO_2 and the V_2O_5/CeO_2-ZrO_2 were less than the V_2O_5/CeO_2-SiO_2. The catalysts also desorb oxygen on oxygen vacancies at higher temperature. Thus, the re-oxidation which is the limiting step for the selective oxidation of H_2S to sulfur element was slower comparing to the V_2O_5/CeO_2-SiO_2 catalyst.

Due to the complex of the H_2S oxidation reaction, SO_2 was also formed by a secondary reaction of sulfur on the catalyst surface [8]. Plotting concentration of SO_2 time profiles showed the SO_2 concentration less than 20 ppm with no change of CO_2 and CH_4 for all the V_2O_5/CeO_2 and V_2O_5/CeO_2-MO_2 catalysts. To confirm the presence of sulfur element product, used catalysts were characterized by EDX and the highest amount of sulfur element was found to deposit on the V_2O_5/CeO_2-SiO_2 at 5.5 wt.% (H_2S conversion ~73%). For the V_2O_5/CeO_2-8 (H_2S conversion ~ 66%) and V_2O_5/CeO_2-8 (H_2S conversion ~ 61%) the elemental sulfur deposited on the catalyst were 4.1 wt.% and 3.9 wt.%, respectively.
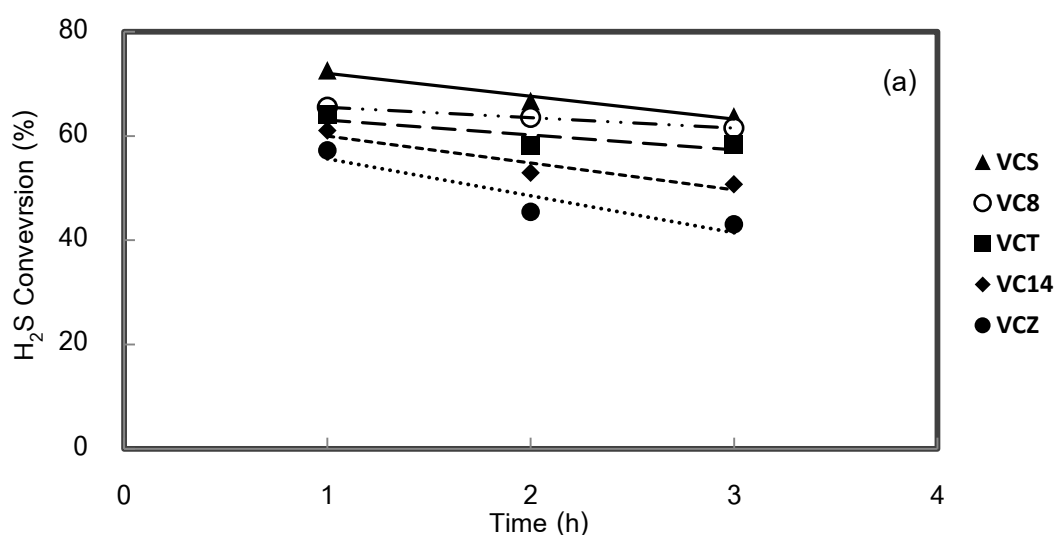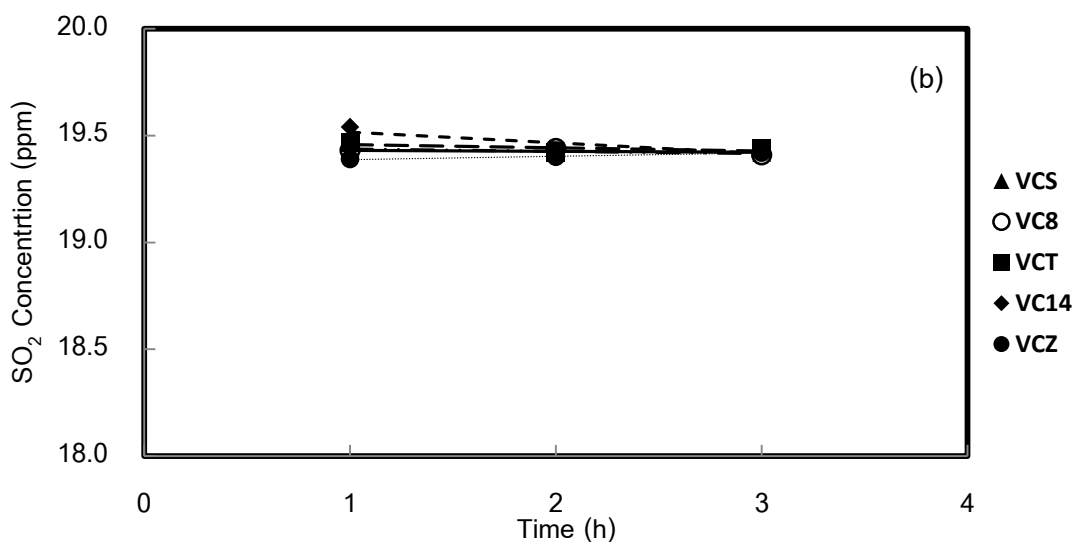
Figure 19 (a) H_2S conversion (b) SO_2 concentration as a function of time of supported V_2O_5 catalyst.

The best catalyst from the first part of the study was selected to study the effect of mixing molar ratios between CeO_2 and MO_2 support on the catalytic performance for selective catalytic oxidation of H_2S. V_2O_5/CeO_2-TiO_2 and V_2O_5/CeO_2-SiO_2 were selected to further study. The molar ratio between CeO_2 and MiO_2 were varied in order: 1:2, 1:3, 2:1 and 3:1. For the case of V_2O_5/CeO_2-TiO_2, the optimum molar ration of VCT was 1:1 in which the catalyst was mostly active among the VCT catalyst series. Higher component of TiO_2 occur two electrons will leave the polarons and will react with the V_2O_5 cluster to form and VO_3^- and VO_2^- result to low activity [47]. From Figure 21, the experiment results showed that V_2O_5/CeO_2-SiO_2 with 1:1 molar ratio base metal oxide exhibited the highest conversion of H_2S among the VCS catalyst series. According to Shin et al. [47], a characteristic of reduced V_2O_5, such as V_2O_3 and V_2O_4 which were found on V_2O_5/SiO_2 affected the re-oxidation to its original V_2O_5 with difficultly. Therefore, higher component of SiO_2 in support disguised good properties of ceria resulting in poor performances of catalyst. Decreasing of H_2S conversion of VCS21 and VCS31 compared with VCS due to the decreasing component of SiO_2 led to low specific surface area.

Plotting concentration of SO_2 time profiles showed the SO_2 concentration less than 20 ppm with no change of CO_2 and CH_4 for all the V_2O_5/CeO_2 and V_2O_5/CeO_2-MO_2 catalysts similar to the previous part.
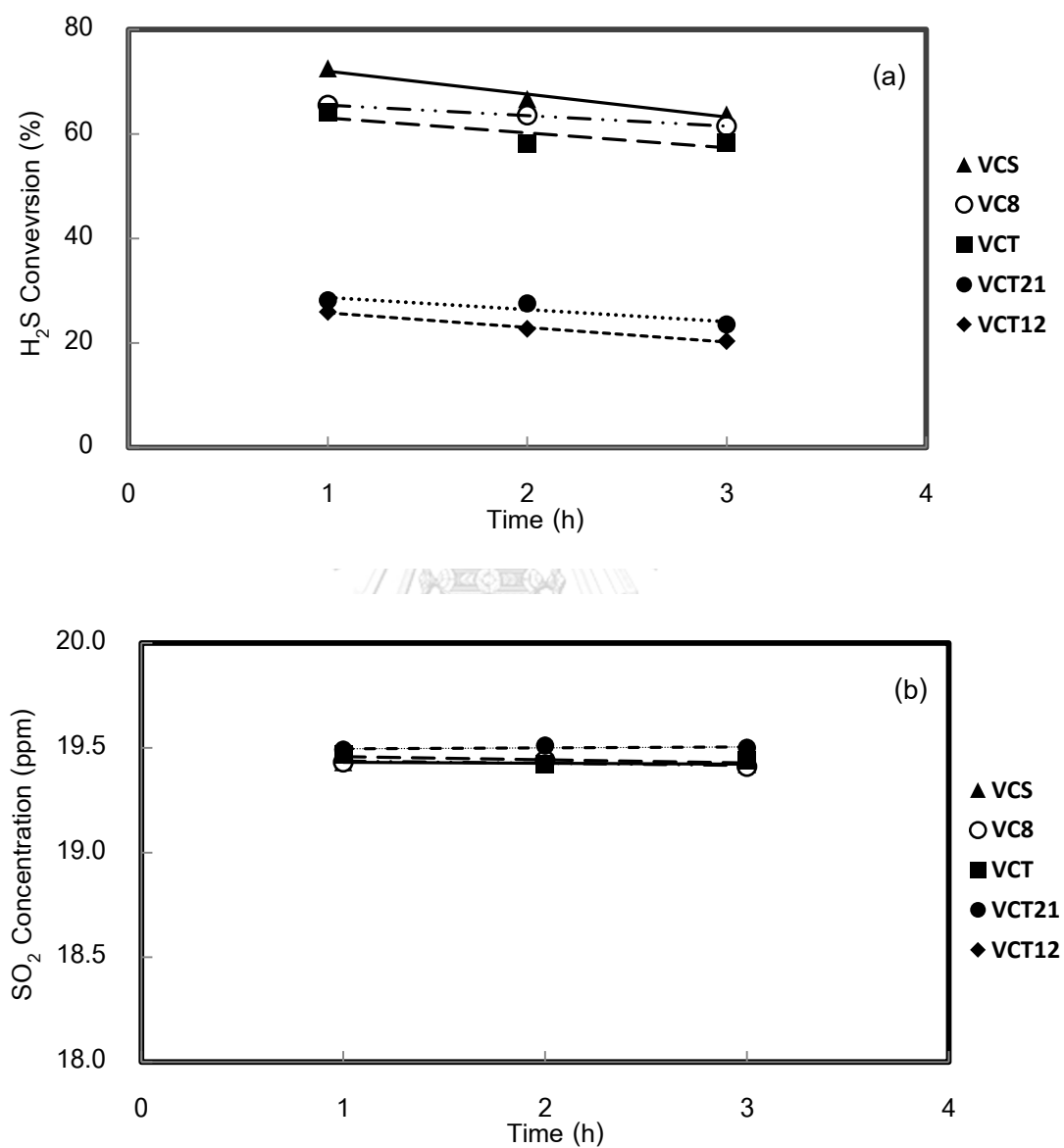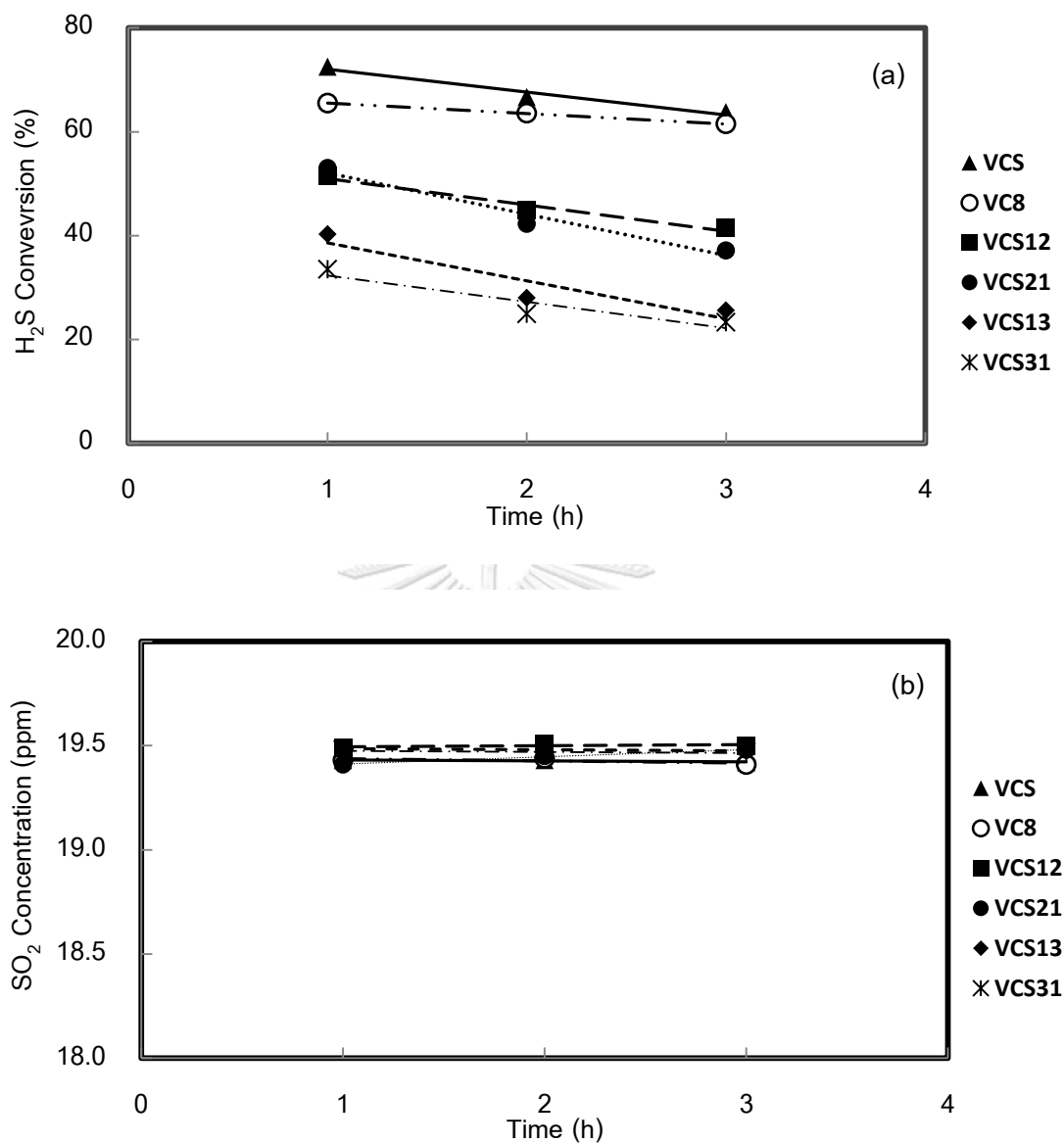

Figure 20 a) H_2S conversion (b) SO_2 concentration as a function of time of supported V_2O_5 catalyst (V_2O_5/CeO_2-TiO_2 series).

Figure 21 a) H$_2$S conversion (b) SO$_2$ conventration as a function of time of supported

V$_2$O$_5$ catalyst (V$_2$O$_5$/CeO$_2$-SiO$_2$ series).

CHAPTER V
CONCLUSIONS AND RECCOMENDATIONS

5.1 Conclusion

The characteristics and catalytic activity of V_2O_5 dispersed on pure CeO_2 and CeO_2-MO_2 mixed oxide supports prepared with different molar ratios between CeO_2 and MO_2 in the selective oxidation of H_2S were reported and discussed. The catalytic activity tests were carried out in H_2S oxidation at 130 $^\circ$C and atmospheric pressure. The characteristics of catalysts were analyzed by XRD, N_2 physisorption, ICP-OES, SEM-EDX, FTIR, and O_2-TPD. Ceria has the ability to capture, store and transfer surface oxygen species which exhibits exceptional redox properties so, presumable supplies active oxygen to V_2O_5 that are reduced during the reaction. It is suggested that interaction between V_2O_5 and support and well dispersion of active site played an importance role in determining the performance of catalysts. From this study, the effect of adding mixed-metal oxide support led to smaller CeO_2 crystallite suggesting the subsistence of a strong interaction between CeO_2 support and the mixed-oxide support. V_2O_5/CeO_2-SiO_2 catalysts exhibited the highest specific surface area, smallest crystallite size, and lowest desorption temperature for adsorption-desorption temperature of oxygen on the oxygen vacancies, indicating the easier desorption of chemically adsorbed oxygen (O_2^{2-}/O^-) on the oxygen vacancies for V_2O_5/CeO_2-SiO_2 as compared to the others catalyst. The highest partial existence of Ce^{3+} on V_2O_5/CeO_2-SiO_2 catalyst also favored the formation of chemically adsorbed oxygen on the oxygen vacancies, which could be the most active oxygen directly affecting the performance of catalyst in the oxidation reaction. In addition, the presence of partially reduced V-Ce may influence the amount of active surface oxygen (O_S) which led to the easier adsorb/desorb oxygen on the oxygen vacancies. V^{4+} with more oxygen vacancies can develop strong redox capability and improved catalytic performance as shown by the higher activity of VC8 comparing to VC14. The products from this reaction are sulfur element and $SO_2 < 20$ ppm with no change of CO_2 and CH_4. It may be applied in H_2S removal from biogas.

5.2 Recommendations

1. The effect of amount dopant on the characteristics and properties of V_2O_5 on supports should be further studied in the selective oxidation of H_2S.

2. The characterization of V_2O_5 catalysts supported on the supports should be analyzed by high resolution analytical techniques because of very low content of dopant.

3. The characterization of mixed-oxide supported catalysts with vary molar ratio should be analyzed by more technique in order to explain and discuss.

4. The stability and catalyst deactivation of catalysts should be further tested.
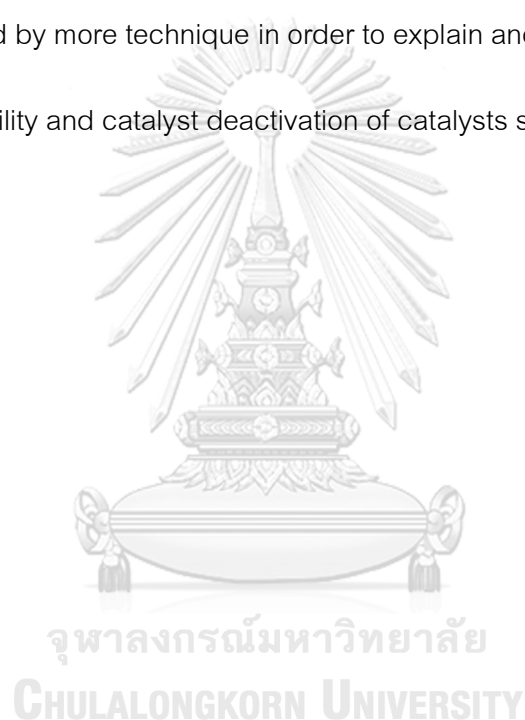
REFERENCES

[1]   Sindhu,R., Binod, P., Pandey, A., Ankaram, S., Duan, Y., and Awasthi, M. K., Biofuel Production From Biomass. *Current Developments in Biotechnology and Bioengineering* 2019, 79-92.

[2]   Chen, X. Y., Vinh-Thang, H., Ramirez, A. A., Rodrigue, D., and Kaliaguine, S., Membrane gas separation technologies for biogas upgrading. *RSC Advances* *2015,* 5(31), 24399-24448.

[3]   Mamun, M. R. A., and Torii, S., Removal of Hydrogen Sulfide (H_2S) from Biogas Using Zero-Valent Iron. *Journal of Clean Energy Technologies* *2015,* 3(6), 428-432.

[4]   Latosov, E., Loorits, M., Maaten, B., Volkova, A., and Soosaar, S., Corrosive effects of H_2S and NH_3 on natural gas piping systems manufactured of carbon steel. *Energy Procedia* *2017,* 128, 316-323.

[5]   Soriano, M. D., Cecilia, J. A., Natoli, A., Jiménez-Jiménez, J., López Nieto, J. M., and Rodríguez-Castellón, E., Vanadium oxide supported on porous clay heterostructure for the partial oxidation of hydrogen sulphide to sulfur. *Catalysis Today* *2015,* 254, 36-42.

[6]   Zhang, X., Dou, G., Wang, Z., Li, L., Wang, Y., Wang, H., and Hao, Z., Selective catalytic oxidation of H_2S over iron oxide supported on alumina-intercalated Laponite clay catalysts. *J Hazard Mater* *2013,* 104-11.

[7]   Fahim, M. A., Al-Sahhaf, T. A., Elkilani, A. S., *Fundamentals of Petroleum Refining* 2015. Elsevier Netherlands.

[8]   Barba, D., Palma, V., and Ciambelli, P., Screening of catalysts for H_2S abatement from biogas to feed molten carbonate fuel cells. *International Journal of Hydrogen Energy* *2013,* 38(1), 328-335.

[9]   Li, K. T., Huang, M. Y., and Cheng, W. D., Vanadium-Based Mixed-Oxide Catalysts for Selective Oxidation of Hydrogen Sulfide to Sulfur. *Industrial & Engineering Chemistry Reserch* *1996,* 35, 621-626.

[10] Davydov, A. A., Marshneva, V. I., and Shepotko, M. L., Metal oxides in hydrogen sulfide oxidation by oxygen and sulfur dioxide. *Applied Catalysis A: General* **2003,** 244(1), 93-100.

[11] Palma, V., and Barba, D., Low temperature catalytic oxidation of H_2S over V_2O_5/CeO_2 catalysts. *International Journal of Hydrogen Energy* **2014,**.39(36), 21524-21530.

[12] Pongthawornsakun, B., Phatyenchuen, S., Panpranot, J., and Praserthdam, P., The low temperature selective oxidation of H_2S to elemental sulfur on TiO_2 supported V_2O_5 catalysts. *Journal of Environmental Chemical Engineering* **2018,** 6(1), 1414-1423.

[13] Zhang, X., Dou, G., Wang, Z., Cheng, J., Wang, H., Ma, C., and Hao, Z., Selective oxidation of H_2S over V_2O_5 supported on CeO_2-intercalated Laponite clay catalysts. *Catalysis Science & Technology* **2013,** 3(10).

[14] Plugge, C. M., Biogas. *Microb Biotechnol* **2017,** 10(5), 1128-1130.

[15] Hydrogen Sulfide (H_2S). *Occupational Safety and Health Administration* **2005**, U. S. Department of Labor.

[16] *H_2S (hydrogen sulfide) Knowledge can save lives* 2014, Drager Safety AG & Co. KGaA United Areb Emirates.

[17] Shin, M. Y., Nam, C. M., Park, D. W., and Chunga, J. S., Selective oxidation of H_2S to elemental sulfur over VO_x/SiO_2 and V_2O_5 catalysts. *Applied Catalysis A: General* **2001**, 213-225.

[18] Bai, Y., and Bai, Q., Subsea Corrosion and Scale. *Subsea Engineering Handbook* 2019, 455-487.

[19] Bineesh, K. V., Kim, D. K., Kim, D. W., Cho, H. J., and Park, D. W., Selective catalytic oxidation of H_2S to elemental sulfur over V_2O_5/Zr-pillared montmorillonite clay. *Energy & Environmental Science* **2010**, 3(3), 302-310.

[20] Brauer, G., Vanadium, Niobium, Tantalum. *Handbook of Preparative Inorganic Chemistry* **1963,** 1, 1270-1272.

[21]   Bauer, G., Guther, V., Hess, H., Otto, A., Roidl, O., Roller, H., and Sattelberger, S., Vanadium and vanadium compounds. *Encyclopedia of Industrial Chemistry* *2003,* 38, 1-21.

[22]   Londero, E., and Schröder, E., Role of van der Waals bonding in the layered oxide V_2O_5: First-principles density-functional calculations. *Physical Review B* *2010,* 82(5).

[23]   Costigan, M., Cary, R., and Dobson, S., Identify and Physical/Chemical Properties. *Vanadium Pentoxide and Other Inorganic Vanadium Compound* *2001,* 7.

[24]   Kim, M. I., Park, D. W., Park, S. W., Yang, X., Choi, J. S., and Suh, D. J., Selective oxidation of hydrogen sulfide containing excess water and ammonia over vanadia–titania aerogel catalysts. *Catalysis Today* *2006,* 111(3-4), 212-216.

[25]   Soriano, M. D., Jiménez-Jiménez, J., Concepción, P., Jiménez-López, A., Rodríguez-Castellón, E., and Nieto, J. M. L., Selective oxidation of H_2S to sulfur over vanadia supported on mesoporous zirconium phosphate heterostructure. *Applied Catalysis B: Environmental* *2009,* 92(3-4), 271-279.

[26]   Scirè, S., and Palmisano, L., Cerium and cerium oxide: A brief introduction. *Cerium Oxide (CeO_2): Synthesis, Properties and Applications* 2020, 1-12.

[27]   Shin, M. Y., Nam, C. M., Park, D. W., and Chung, J. S., Selective oxidation of H_2S to elemental sulfur over VO_x/SiO_2 and V_2O_5 catalysts. *Applied Catalysis A: General* *2001,* 211, 213-225.

[28]   Yasyerli, S., Dogu, G., and Dogu, T., Selective oxidation of H_2S to elemental sulfur over Ce–V mixed oxide and CeO_2 catalysts prepared by the complexation technique. *Catalysis Today* *2006,* 117(1-3), 271-278.

[29]   Reddy, B. M., Lakshmanan, P., and Khan, A., Investigation of Surface Structures of Dispersed V_2O_5 on CeO_2-SiO_2, CeO_2-TiO_2, and CeO_2-ZrO_2 Mixed Oxides by XRD, Raman, and XPS Techniques. *The Journal of Physical Chemistry B* *2004,* 108, 16855-16863.

[30] Reddy, B. M., and Khan, A., Surface Characterization of CeO_2/SiO_2 and $V_2O_5/CeO_2/SiO_2$ Catalysts by Raman, XPS, and Other Techniques. *The Journal of Physical Chemistry B* **2002,** 106, 10964-10972.

[31] Kang, D. H., Kim, M. I., and Park, D. W., Selective oxidation of H_2S to sulfur over CeO_2-TiO_2 catalyst. *Korean Journal of Chemical Engineering* **2016,** 33(3), 838-843,.

[32] Palma, V., Barba, D., and Ciambelli, P., Selective Oxidation of H_2S to Sulphur from Biogas on V_2O_5/CeO_2 Catalysts. *Chemical Engineering Transactions* **2013,** 32, 631-636.

[33] Gu, X., Ge, J., Zhang, H., Auroux, A., and Shen, J., Structural, redox and acid–base properties of V_2O_5/CeO_2 catalysts. *Thermochimica Acta* **2006,** 451(1-2), 84-93.

[34] Gannoun, C., Delaigle, R., Debecker, D. P., Eloy, P., Ghorbel, A., and Gaigneaux, E. M., Effect of support on V_2O_5 catalytic activity in chlorobenzene oxidation. *Applied Catalysis A: General* **2012,** 447-448, 1-6.

[35] Preuss, A., and Gruehn, R., Preparation and Structure of Cerium Tatantes Ce_2TiO_5, $Ce_2Ti_2O_7$ and $Ce_4Ti_9O_{24}$. *Journal od Solid Atate Chemistry* **1994,** 110, 363-369.

[36] Lin, J., and Yu, J. C., An investigation on photocatalytic activities of mixed TiO,-rare earth oxides for the oxidation of acetone in air. *Journal of Photochemistry and Photobiology A: Chemistry* **1998,** 116, 63-67.

[37] Reddy, B. M., and Khan, A., Nanosized CeO_2–SiO_2, CeO_2–TiO_2, and CeO_2–ZrO_2 Mixed Oxides: Influence of Supporting Oxide on Thermal Stability and Oxygen Storage Properties of Ceria. *Catalysis Surveys from Asia* **2005,** 9(3), 155-171.

[38] Tian, W., Yin, J., Wei, L., Shen, Q., Bibi, R., Liu, M., Yang, B., Li, N., and Zhou, J., Hydrothermally prepared nanosized and mesoporous $Ce_{0.4}Zr_{0.6}O_2$ solid solutions with shape dependence in photocatalysis for the degradation of methylene blue. *RSC Advances* **2017,** 7(28), 17020-17029.

[39]   Bosco, M. V., Bañares, M. A., Martínez-Huerta, M. V., Bonivardi, A. L., and Collins, S. E., In situ FTIR and Raman study on the distribution and reactivity of surface vanadia species in V_2O_5/CeO_2 catalysts. *Journal of Molecular Catalysis A: Chemical* **2015,** 408, 75-84.

[40]   Farahmandjou, M., and Zarinkamar, M., Synthesis of nano-sized ceria (CeO_2) particles via a cerium hydroxy carbonate precursor and the effect of reaction temperature on particle morphology. *Journal of Ultrafine Grained and Nanostructured Materials* **2015,** 48, 5-10.

[41]   Babitha, K. K., Sreedevi, A., Priyanka, K. P., Sabu, B., and Varghese, T., Structure Characterization and Optical Studies of CeO_2 Nanaoparticles Synthesized by Chemical Precipitation. *Indian Journal of pure & Applied Physics* **2015,** 53, 596-603.

[42]   Farahmandjou, M., Zarinkamar, M., and Firoozabadi, T. P., Synthesis of Cerium Oxide (CeO_2) nanoparticles using simple CO-precipitation method. *Revista Mexicana de F´ısica* **2016,** 62, 496-499.

[43]   Bagheri, S., Shameli, K., and Abd Hamid, S. B., Synthesis and Characterization of Anatase Titanium Dioxide Nanoparticles Using Egg White Solution via Sol-Gel Method. *Journal of Chemistry* **2013,** 2013, 1-5.

[44]   Yu, J. C., Zhang, L., Zheng, Z., and Zhao, J., Synthesis and Characterization of Phosphated Mesoporous Titanium Dioxide with High Photocatalytic Activity. *Chemistry Mater* **2003,** 15, 2280-2286.

[45]   Singh, A. K., and Nakate, U. T., Microwave synthesis, characterization, and photoluminescence properties of nanocrystalline zirconia. *Scientific Worl dJournal* **2014**, 2014, 349-457.

[46]   Vivekanandhan, S., Venkateswarlu, M., Rawls, H. R., and Satyanarayana, N., Acrylamide assisted polymeric citrate route for the synthesis of nanocrystalline ZrO_2 powder. *Materials Chemistry and Physics* **2010,** 120(1), 148-154.

[47]   Kristoffersen, H. H., Neilson, H. L., Buratto, S. K., and Metiu, H., Stability of V_2O_5 Supported on Titania in the Presence of Water, Bulk Oxygen Vacancies, and Adsorbed Oxygen Atoms. *The Journal of Physical Chemistry C* **2017,** 121(15), 8444-8451.

[48]   An, Z., Zhuo, Y., Xu, C., and Chen, C., Influence of the TiO_2 crystalline phase of MnO_x/TiO_2 catalysts for NO oxidation. *Chinese Journal of Catalysis* **2014,** 35(1), 120-126.

[49]   Song, D., Shao, X., Yuan, M., Wang, L., Zhan, W., Guo, Y., Guo, Y., and Lu, G., Selective catalytic oxidation of ammonia over MnO_x–TiO_2 mixed oxides. *RSC Advances* **2016,** 6(91), 88117-88125.

[50]   Liu, Y., Jiang, C., Chu, W., Sun, W., and Xie, Z., Novel F–V_2O_5/SiO_2 catalysts for oxidative dehydrogenation of propane. *Reaction Kinetics, Mechanisms and Catalysis* **2010,** 101(1), 141-151.

[51]   Zhu, H., Qin, Z., Shan, W., Shen, W., and Wang, J., "Low-temperature oxidation of CO over Pd/CeO_2–TiO_2 catalysts with different pretreatments. *Journal of Catalysis* **2005,** 233(1), 41-50.

[52]   Kugai, J., Subramani, V., Song, C., Engelhard, M., and Chin, Y., "\Effects of nanocrystalline CeO_2 supports on the properties and performance of Ni–Rh bimetallic catalyst for oxidative steam reforming of ethanol. *Journal of Catalysis* **2006,** 238(2), 430-440.

[53]   Kundakovic, L., and Flytzani-Stephanopoulos, M., Cu- and Ag-Modified Cerium Oxide Catalysts for Methane Oxidation. *Journal of catalysis* **1998,** 179, 203-221.

APPENDIX A

CALCULATION FOR CATALYST PREPARATION

A1. Calculation for the CeO_2-TiO_2 support preparation (1:1 molar ratio base on oxide)

Chemical information

Cerium (III) nitrate hexahydate, 99.5% M_w = 434.22 g/mol

Titanium (IV) butoxide, 97% M_w = 340.32 g/mol

Calculation

To preparation 1:1 molar ratio base on oxide of CeO_2-TiO_2 support following:

- Desire CeO_2 0.0086 mole

- Desire TiO_2 0.0086 mole

Prepare $Ce(NO_3)_3 \cdot 6H_2O$ for CeO_2 0.0086 mole

$$0.0086 \text{ mole } CeO_2 \times \frac{1 \text{ mole } Ce(NO_3)_3 6H_2O}{0.995 \text{ mole } Ce} \times \frac{1 \text{ mole } Ce}{1 \text{ mole } CeO_2} = 0.00864 \text{ mole } Ce(NO_3)_3 \cdot 6H_2O$$

$$0.00864 \text{ mole } Ce(NO_3)_3 6H_2O \times \frac{434.22 \text{ g } Ce(NO_3)_3 6H_2O}{1 \text{ mole } Ce(NO_3)_3 6H_2O} = 3.75 \text{ g } Ce(NO_3)_3 \cdot 6H_2O$$

Prepare $Ti(C_4H_9O)_4$ for TiO_2 0.0086 mole

$$0.0086 \text{ mole } TiO_2 \times \frac{1 \text{ mole } Ti(C_4H_9O)_4}{0.97 \text{ mole } TiO_2} = 0.0089 \text{ mole } Ti(C_4H_9O)_4$$

$$0.0089 \text{ mole } Ti(C_4H_9O)_4 \times \frac{340.32 \text{ g } Ti(C_4H_9O)_4}{1 \text{ mole } Ti(C_4H_9O)_4} = 3.02 \text{ g } Ti(C_4H_9O)_4$$

So, for preparation of CeO_2-TiO_2 support, used 3.75 g $Ce(NO_3)_3 \cdot 6H_2O$ and 3.02 g $Ti(C_4H_9O)_4$

A2. Calculation for the CeO$_2$-SiO$_2$ support preparation (1:1 molar ratio base on oxide)

Chemical information

Ammonium cerium (IV) nitrate: Ce(NH$_4$)$_2$(NO$_3$)$_6$, 99.99%   M$_w$ = 548.22 g/mol

Colloidal silica 40%in water, ρ = 1.3 g/ml   M$_w$ = 60.08 g/mol

Calculation

To preparation 1:1 molar ratio base on oxide of CeO$_2$-SiO$_2$ support following:

- Desire CeO$_2$ 0.0086 mole

- Desire SiO$_2$ 0.0086 mole

Prepare Ce(NH$_4$)$_2$(NO$_3$)$_6$ for CeO$_2$ 0.0086 mole

$$0.0086 \text{ mole CeO}_2 \times \frac{1 \text{ mole Ce(NH}_4)_2(\text{NO}_3)_6}{0.9999 \text{ mole Ce}} \times \frac{1 \text{ mole Ce}}{1 \text{ mole } CeO_2} = 0.0086 \text{ mole Ce(NH}_4)_2(\text{NO}_3)_6$$

$$0.0086 \text{ mole Ce(NH}_4)_2(\text{NO}_3)_6 \times \frac{548.22 \text{ g Ce(NH}_4)_2(\text{NO}_3)_6}{1 \text{ mole Ce(NH}_4)_2(\text{NO}_3)_6} = 4.71 \text{ g Ce(NH}_4)_2(\text{NO}_3)_6$$

Prepare colloidal silica for SiO$_2$ 0.0086 mole

$$0.0086 \text{ mole SiO}_2 \times \frac{1 \text{ mole colloidal silica}}{0.4 \text{ mole } SiO_2} = 0.0215 \text{ mole colloidal silica}$$

$$0.0215 \text{ mole } colloidal\ silica \times \frac{60.08 \text{ g colloidal silica}}{1 \text{ mole colloidal silica}} \times \frac{ml}{1.3\ g} = 0.99 \text{ ml colloidal silica}$$

So, for preparation of CeO$_2$-SiO$_2$ support, used 4.71 g Ce(NH$_4$)$_2$(NO$_3$)$_6$ and 0.99 ml colloidal silica

A3. Calculation for the CeO_2-ZrO_2 support preparation (1:1 molar ratio base on oxide)

Chemical information

    Cerium (III) nitrate hexahydate, 99.5% M_w = 434.22 g/mol

    Zirconium (IV) oxynitrate hydrate, 99% M_w = 231.23 g/mol

Calculation

    To preparation 1:1 molar ratio base on oxide of CeO_2-ZrO_2 support following:

    - Desire CeO_2 0.0086 mole

    - Desire ZrO_2 0.0086 mole

Prepare $Ce(NO_3)_3 \cdot 6H_2O$ for CeO_2 0.0086 mole

$$0.0086 \text{ mole } CeO_2 \times \frac{1 \text{ mole } Ce(NO_3)_3 6H_2O}{0.995 \text{ mole } Ce} \times \frac{1 \text{ mole } Ce}{1 \text{ mole } CeO_2} = 0.00864 \text{ mole } Ce(NO_3)_3 \cdot 6H_2O$$

$$0.00864 \text{ mole } Ce(NO_3)_3 6H_2O \times \frac{434.22 \text{ g } Ce(NO_3)_3 6H_2O}{1 \text{ mole } Ce(NO_3)_3 6H_2O} = 3.75 \text{ g } Ce(NO_3)_3 \cdot 6H_2O$$

Prepare $ZrO(NO_3)_2 \cdot 2H_2O$ for ZrO_2 0.0086 mole

$$0.0086 \text{ mole } ZrO_2 \times \frac{1 \text{ mole } ZrO(NO_3)_2 2H_2O}{0.99 \text{ mole } ZrO_2} = 0.0087 \text{ mole } ZrO(NO_3)_2 \cdot 2H_2O$$

$$0.0087 \text{ mole } ZrO(NO_3)_2 2H_2O \times \frac{231.23 \text{ g } ZrO(NO_3)_2 2H_2O}{1 \text{ mole } ZrO(NO_3)_2 2H_2O} = 2.01 \text{ g } ZrO(NO_3)_2 \cdot 2H_2O$$

So, for preparation of CeO_2-ZrO_2 support, used 3.75 g $Ce(NO_3)_3 \cdot 6H_2O$ and 2.01 g $ZrO(NO_3)_2 \cdot 2H_2O$

A4. Calculation for the 3 wt.% V_2O_5/CeO_2 catalyst preparation

Chemical information

Ammonium metavanadate, 99.99% M_w = 116.98 g/mol

Vanadium pentoxide M_w = 181.88 g/mol

Cerium (IV) oxide M_w = 172.115 g/mol

Calculation

To preparation 3 wt.% V_2O_5/CeO_2 catalyst follow:

- Desire CeO_2 2 g

- Desire V_2O_5 3 wt.%

For 3 wt.% V_2O_5/CeO_2 100 g

Consist of CeO_2 97 g V_2O_5 3 g

If CeO_2 2 g V_2O_5 = 2 g CeO_2 $\times \dfrac{3 \text{ g } V_2O_5}{97 \text{ g } CeO_2}$ = 0.062 g V_2O_5

Prepare NH_4VO_3 for V_2O_5 0.062 g

0.062 g $V_2O_5 \times \dfrac{1 \text{ mole } V_2O_5}{181.88 \text{ g } V_2O_5}$ = 0.00341 mole V_2O_5

0.00341 mole $V_2O_5 \times \dfrac{2 \text{ mole } NH_4VO_3}{1 \text{ mole } V_2O_5}$ = 0.00682 mole NH_4VO_3

0.00682 mole $NH_4VO_3 \times \dfrac{116.98 \text{ g } NH_4VO_3}{1 \text{ mole } NH_4VO_3} \times \dfrac{1}{0.9999}$ = 0.80 g NH_4VO_3

So, for preparation of 3 wt.% V_2O_5/CeO_2 catalyst, used 2 g CeO_2 and 0.80 g NH_4VO_3

APPENDIX B

CALCULATION OF THE CRYSTALLITE SIZE

B1. Calculation of the crystallite size of CeO$_2$ by using Debye – Scherrer's equation

The average crystal size of CeO$_2$ used Scherrer's equation to calaulate from FWHM (full width at half maximum) of XRD peak corresponding crystalline of CeO$_2$ at 2 theta ~ 28.6° follow equeation:

$$D = \frac{K\lambda}{\beta cos\theta}$$

Where;

D	=	Crystallite size, Å
K	=	Crystallite-shape factor (= 0.9 for FWHM of spherical crystals with cubic symmetry)
λ	=	the X-ray wavelength, 1.5418 Å for CuK_α
β	=	X-ray diffraction broadening, radian
θ	=	Observes peak angel, degree

Example

Calculation of the crystallite size of CeO$_2$ (< 25 nm, supplier: Sigma Aldrich)

Information   The major peak of CeO$_2$ was observed at 2 theta ~ 28.55°

The half-height width of the diffraction peak at 28.55° = 0.42°

Calculation   28.55° to radian   = $\dfrac{28.55(2\pi)}{360}$ = 0.5 radian

0.42° to radian   = $\dfrac{0.42(2\pi)}{360}$ = 0.0073 radian

$$
\begin{aligned}
D &= \frac{K\lambda}{\beta cos\theta} \\
&= \frac{0.9(1.5418)}{0.0073 \cos 0.5} \\
&= 190.1 \text{ Å} \\
&= 19 \text{ nm}
\end{aligned}
$$

APPENDIX C

CALIBRATION CURVE

The calibration curve is used to calculate a concentration of substance. It is created from area which analyzed by injecting the standard gas at different volumes into GC (gas chromatography). Ploting graph between peak area at different concentrations (x-axis) and mole or concentration of gas (y-axis).

$$y = 1E\text{-}08x + 19.293$$

$$R^2 = 0.9801$$
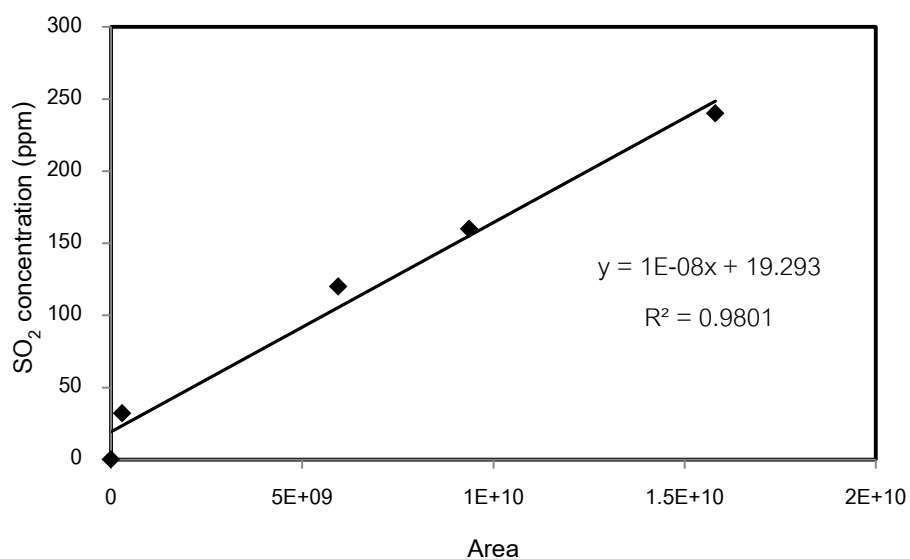
Figure 22 Calibration curve of sulfur dioxide (SO_2).

APPENDIX D

SEM IMAGE OF CATALYSTS
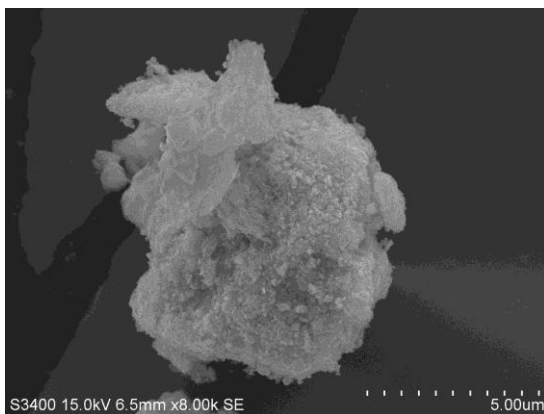
Figure 22 SEM image of VC8
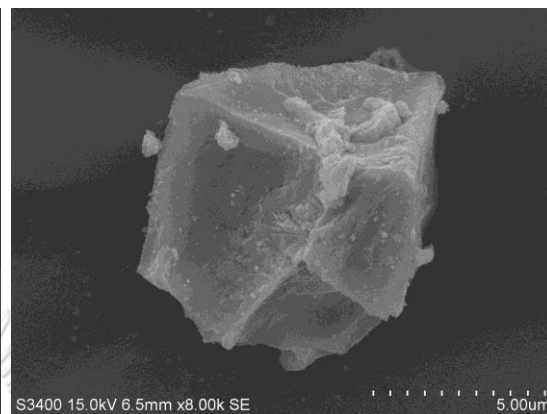
Figure 23 SEM image of VC14
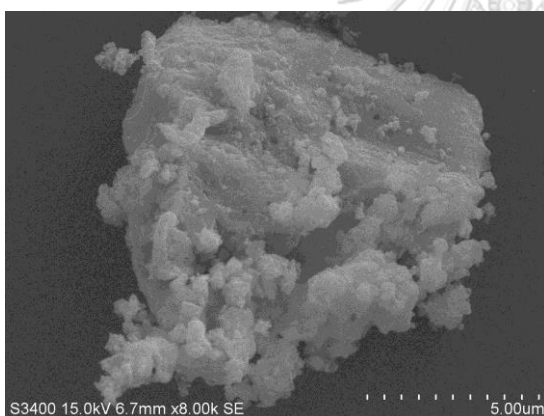
Figure 24 SEM image of VCT
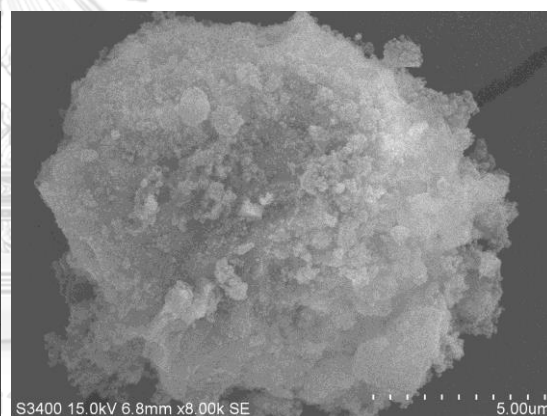
Figure 25 SEM image of VCS
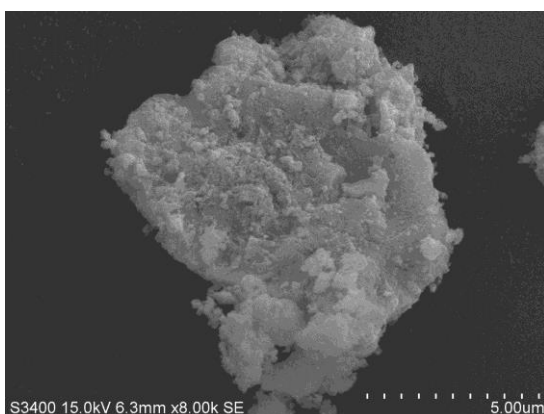
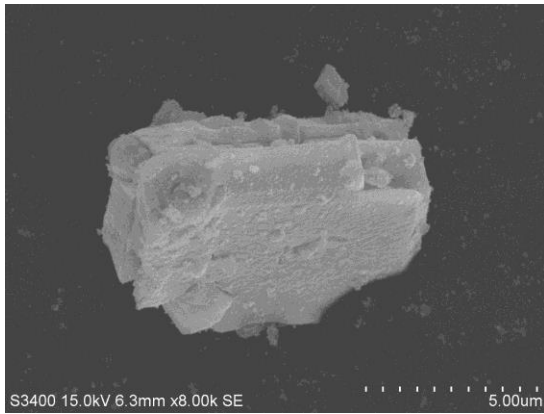Figure 26 SEM image of VCZ
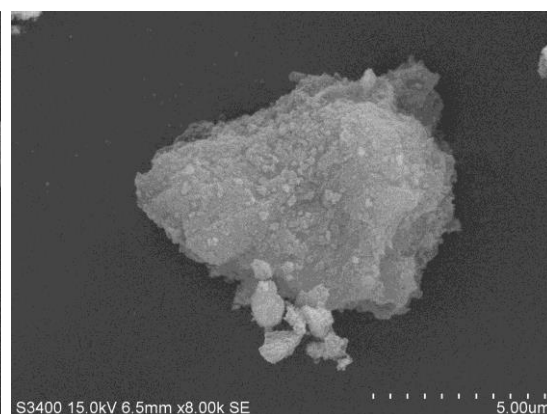
Figure 27 SEM image of VCS12

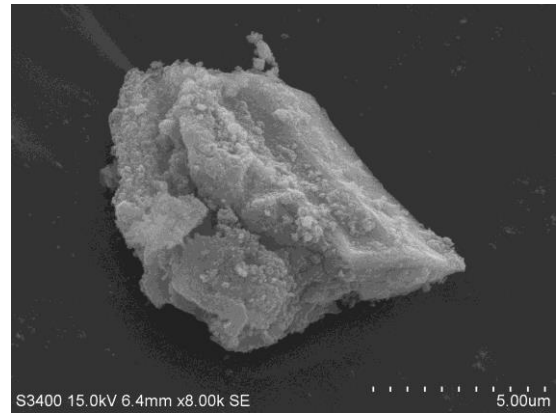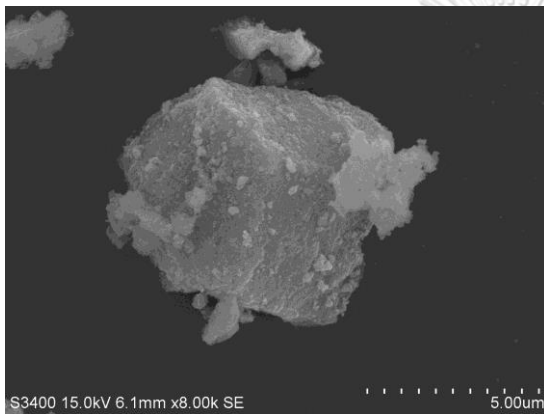Figure 28 SEM image of VCS13

Figure 29 SEM image of VCS21

Figure 30 SEM image of VCS31
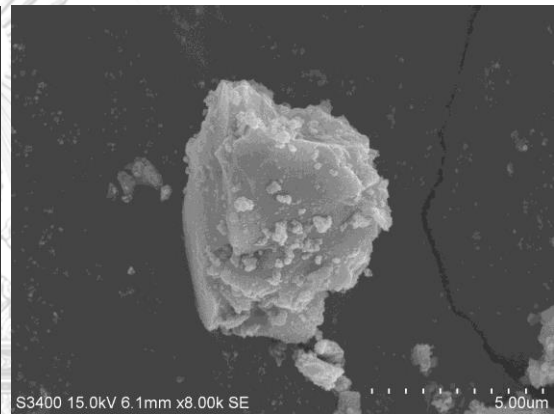

Figure 31 SEM image of VCT12
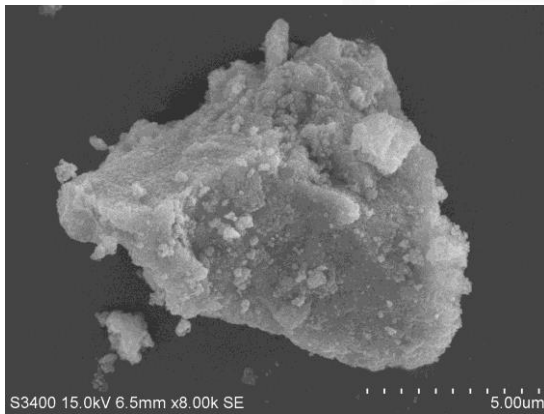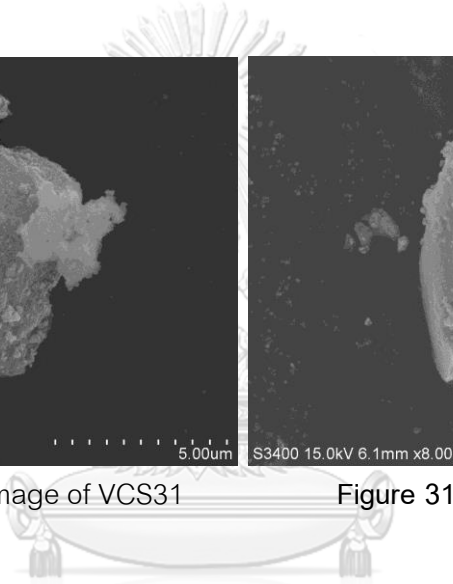

Figure 32 SEM image of VCT21

VITA

NAME   Benjamaporn Tudkesorn

DATE OF BIRTH   28 September 1995

PLACE OF BIRTH   Suphanburi

INSTITUTIONS ATTENDED   Bachelor Degree of Chemical Engineering from Faculty of
                         Engineering, King Mongkut Institute of Technology
                         Ladkrabang, Thailand 2018.
                         Continuous study in Master Degree of Chemical
                         Engineering, Faculty of Engineering, Chulalongkorn
                         University, Thailand in August 2018.

HOME ADDRESS   41 Moo 6 Hua Khao Sub-district, Doembangnangbuat
                         District,Suphanburi Thailand 72120

จุฬาลงกรณ์มหาวิทยาลัย
CHULALONGKORN UNIVERSITY